Purging viral latency by a bifunctional HSV-vectored therapeutic vaccine in chronically SIV-infected macaques

Ziyu Wen,[1#] Pingchao Li,[2#] Yue Yuan,[1#] Congcong Wang,[1#] Minchao Li,[1] Haohang Wang,[1] Minjuan Shi,[1] Yizi He,[2] Mingting Cui,[1] Ling Chen,[2*] Caijun Sun,[1,3,4,5*]

[1]School of Public Health (Shenzhen), Sun Yat-sen University, Shenzhen, China;
[2]State Key Laboratory of Respiratory Disease, Guangzhou Institutes of Biomedicine and Health (GIBH), Chinese Academy of Sciences, Guangzhou, China;
[3]Key Laboratory of Tropical Disease Control (Sun Yat-sen University), Ministry of Education, Guangzhou, China;
[4]Shenzhen Key Laboratory of Pathogenic Microbes and Biosafety, Shenzhen campus of Sun Yat-sen University, Shenzhen, China;
[5]State Key Laboratory of Anti-Infective Drug Discovery and Development, School of Pharmaceutical Sciences, Sun Yat-sen University, Guangzhou, China.

#These authors contributed equally to this work.
* For correspondence:
Caijun Sun, suncaijun@mail.sysu.edu.cn (CS);
Ling Chen, chen_ling@gibh.ac.cn (LC)

Abstract

The persistence of latent viral reservoirs remains the major obstacle to eradicating human immunodeficiency virus (HIV). We herein found that ICP34.5 can act as an antagonistic factor for the reactivation of HIV latency by herpes simplex virus type I (HSV-1), and thus recombinant HSV-1 with ICP34.5 deletion could more effectively reactivate HIV latency than its wild-type counterpart. Mechanistically, HSV-ΔICP34.5 promoted the phosphorylation of HSF1 by decreasing the recruitment of protein phosphatase 1 (PP1α), thus effectively binding to the HIV LTR to reactivate the latent reservoirs. In addition, HSV-ΔICP34.5 enhanced the phosphorylation of IKKα/β through the degradation of IκBα, leading to p65 accumulation in the nucleus to elicit NF-κB pathway-dependent reactivation of HIV latency. Then, we constructed the recombinant HSV-ΔICP34.5 expressing simian immunodeficiency virus (SIV) env, gag, or the fusion antigen sPD1-SIVgag as a therapeutic vaccine, aiming to achieve a functional cure by simultaneously reactivating viral latency and eliciting antigen-specific immune responses. Results showed that these constructs effectively elicited SIV-specific immune responses, reactivated SIV latency, and delayed viral rebound after the interruption of antiretroviral therapy (ART) in chronically SIV-infected rhesus macaques. Collectively, these findings provide insights into the rational design of HSV-vectored therapeutic strategies for pursuing an HIV functional cure.

Keywords: HIV, SIV, HSV, therapeutic vaccine, functional cure

Introduction

The epidemic of acquired immunodeficiency syndrome (AIDS), caused by human immunodeficiency virus type I (HIV-1), is still a huge challenge for global public health, with approximately 39 million people living with HIV-1 as of 2022. To date, there is neither a curable drug nor a prophylactic vaccine for clinical use against HIV-1 infections (Sun et al., 2023b, Sun et al., 2023a). Antiretroviral therapy (ART) can effectively control HIV-1 replication to an undetectable level, but the termination of ART usually results in prompt viral rebound from latent viral reservoirs (Archin et al., 2014, Looker et al., 2017, Calistri et al., 2003, Heng et al., 1994). Thus, it is of great priority to explore novel strategies for curing HIV latency. The “Shock and Kill” strategy is considered a promising approach for purging HIV-1 reservoirs, involving the activation of latently infected cells to express viral products (Shock), followed by viral cytopathic effects or specific cytolytic T lymphocytes (CTLs) to eliminate the activated cells (Kill) (Wu et al., 2022, Yang et al., 2019, Kim et al., 2018). Numerous latency-reversing agents (LRAs) (Yang et al., 2019, Wu et al., 2022), including methylation inhibitors, histone deacetylase (HADC) inhibitors (Archin et al., 2017, Lehrman et al., 2005), and bromodomain and extra terminal domain (BET) protein inhibitors (Li et al., 2013, Bisgrove et al., 2007), have been identified to reactivate latent HIV-1 in preclinical studies, but there is no ideal LRA available for clinical patients yet.

Herpes simplex virus (HSV), a human herpesvirus, features a 152-kb double-stranded DNA genome encoding over 80 proteins (Poh, 2016). Owing to its distinctive genetic background, high capacity, broad tropism, thermostability, and

excellent safety profile, the modified HSV constructs have extensive applications in gene therapy and oncolytic virotherapy. For example, talimogene laherparepvec (T-VEC), an HSV-1 variant with ICP34.5 deletion and GM-CSF insertion, received FDA approval in 2015 for treating malignant melanoma, showcasing notable safety and efficacy in clinical practice. Recombinant HSV-based constructs have also emerged as efficacious gene delivery vectors against infectious diseases. Early studies indicated that prophylactic vaccines based on HSV, expressing simian immunodeficiency virus (SIV) antigens, could elicit robust antigen-specific CTL responses in mice and monkeys, providing enduring and partial protection against pathogenic SIVmac239 challenges (Kaur et al., 2007, Murphy et al., 2000). Moreover, increasing data suggest the crucial role of HIV-specific CTL in controlling viral replication and eliminating potential HIV reservoirs (Collins et al., 2020, Leitman et al., 2017). Significantly, epidemiological research suggests a synergistic effect between HSV and HIV infections, with HSV infection in HIV patients being associated with increased HIV-1 viral load and disease progression (Looker et al., 2017, Calistri et al., 2003, Heng et al., 1994). Some studies have further unveiled the ability of HSV to activate HIV latent reservoirs (Amici et al., 2004, Amici et al., 2001, Pierce et al., 2023). Given the potential of HSV to simultaneously induce antigen-specific immune responses and reactivate latent viral reservoirs, we propose a proof-of-concept strategy to achieve an HIV functional cure using a modified bifunctional HSV-vectored therapeutic vaccine.

Results

The modified HSV-ΔICP34.5-based constructs reactivated HIV latency more efficiently than wild-type HSV counterparts

The J-Lat 10.6 cell line, derived from Jurkat T cells containing latent HIV-1 provirus, was infected with wild-type HSV-1 Mckrae strain at different multiplicities of infection (MOI) to assess its capability to reactivate HIV latency. Flow cytometry analysis showed a dose-dependent increase in green fluorescent protein (GFP) expression (*Figure 1A*), indicating that HSV-1 can reactivate latent HIV. Subsequently, we infected J-Lat 10.6 cells with an HSV-1 17 strain containing GFP (HSV-GFP) and observed a significant upregulation in the mRNA levels of HIV-1 driven transcripts, including Tat, Gag, Vif, and Vpr, along with 5'-LTR-containing RNA. This demonstrates that the attenuated HSV-1 strain can reactivate latent HIV at different MOIs (*Figure 1B*). Using the bacterial artificial chromosome (BAC)/galactokinase (galK) system, we then constructed the recombinant HSV deleted with ICP34.5 (HSV-ΔICP34.5) based on HSV-GFP. Notably, we discovered for the first time that the HSV-ΔICP34.5 reactivated HIV latency more efficiently than its parental strain (HSV-GFP). Specifically, the mRNA levels of HIV-1 transcripts, including those driven by the 5' LTR, as well as Tat, Gag, Vpr, Vif were significantly higher in J-Lat 10.6 cells infected with HSV-ΔICP34.5 compared to those treated with HSV-GFP (*Figure 1C*), despite the weaker replication ability of HSV-ΔICP34.5 in these cells, as indicated by the mRNA level of HSV UL27 (*Figure 1D, Figure S1*).

Furthermore, this finding was validated in ACH-2 cells, which are derived from T cells latently infected with replication-competent HIV-1. A significantly higher level of p24 protein, a key indicator of HIV replication, was found in the HSV-ΔICP34.5-infected ACH-2 cells compared to HSV-GFP-treated cells (*Figure 1E*). Additionally, the mRNA levels of HIV-related transcripts, including those driven by the 5' LTR, as well as Tat, Gag, Vpr, Vif, were also significantly increased (*Figure 1F*). Subsequently, we generated J-Lat 10.6 cells stably expressing ICP34.5-Flag-Tag (J-Lat 10.6-ICP34.5) using a recombinant lentivirus system and confirmed the expression of the ICP34.5 protein. Our research revealed that HSV-ΔICP34.5 displayed a reduced capacity to reverse HIV latency in J-Lat 10.6-ICP34.5 cells compared to J-Lat 10.6 cells (*Figure 1G*). Moreover, in J-Lat 10.6-ICP34.5 cells, the potency of latent reversal agents such as phorbol 12-myristate 13-acetate (PMA) and TNF-α was notably reduced when contrasted with J-Lat 10.6 cells (*Figure 1H*). We also confirmed the enhanced reactivation of HIV latency by HSV-ΔICP34.5 in primary $CD4^+$ T cells from people living with HIV (PLWH) (*Figure S2*). In addition, HSV-ΔICP34.5 induced a lower level of inflammatory cytokines (including IL-6, IL-1β, and TNF-α) in primary $CD4^+$ T cells from PLWH compared to HSV-GFP stimulation, likely due to its lower virulence and replication ability (*Figure 1I-K*). Thus, these data suggested that the safety of HSV-ΔICP34.5 in PLWH might be tolerable, at least *in vitro*. In addition, neither adenovirus nor vaccinia virus was able to reactivate HIV latency in this study (Figure S3), and the deletion of ICP0 gene from HSV-1 diminished its reactivation effect on HIV latency (Figure S4). Importantly, overexpressing ICP0 greatly reactivates latent HIV

(Figure S5), implying that this reactivation is virus-specific and that ICP0 plays an important role in reversing HIV latency. Overall, these findings indicated that the recombinant HSV-ΔICP34.5 construct specifically reactivated HIV latency with high efficiency in the presence of ICP0.

The modified HSV-based constructs effectively reactivated HIV latency by modulating the IKKα/β-NF-κB pathway and PP1-HSF1 pathway

Next, based on RNA-seq analysis for HSV-Δ ICP34.5-induced signaling pathways (Figure S6) and previous literature, we explored the mechanism of reactivating viral latency by HSV-ΔICP34.5-based constructs. J-Lat10.6 cells were infected with HSV-GFP or HSV-ΔICP34.5, and results showed that HSV-ΔICP34.5 significantly enhanced the phosphorylation of IKKα/β, promoted the degradation of IKBα, and thus led to the accumulation of p65 in the nucleus (*Figure 2A*). NF-κB is a well-known host transcription factor that exists in the form of the NF-κB-IκB complex in resting cells, but IκB can degrade and release the NF-κB dimer to enter the nucleus and promote gene transcription in response to external stimulation. Using the coimmunoprecipitation (Co-IP) assay, we verified that the ICP34.5 protein had a specific interaction with IKKα/β, and then ICP34.5 could dephosphorylate IKKα/β. Moreover, the overexpression of ICP34.5 effectively inhibited lipopolysaccharide (LPS) -induced NF-κB pathway activation by inhibiting p65 entry into the nucleus (*Figure 2B-C*).

To further clarify the underlying mechanism, we performed the immunoprecipitation-mass spectrometry (IP-MS) analysis in ICP34.5 overexpressing cells to identify other potential molecules contributing to this reactivation, and we found that ICP34.5 can also interact with heat shock 1 protein (HSF1) (*Table S1*). HSF1 has been reported as a transcription factor correlated with the reactivation of HIV latency (Xu et al., 2022, Lin et al., 2018, Zeng et al., 2017). To test whether HSF1 contributes to the reactivation of HIV latency by HSV-ΔICP34.5-based constructs, KRIBB11, an inhibitor of HSF1, was administered to HSV-ΔICP34.5-infected J-Lat 10.6 cells. The results indicated that the reactivation ability of HSV-ΔICP34.5 was significantly inhibited by KRIBB11 treatment in a dose-dependent manner (*Figure 2D-E*). Furthermore, a significant enhancement of the binding of HSF1 to the HIV LTR was observed upon HSV-ΔICP34.5 infection, leading to an increase in the reactivation of HIV latency (*Figure 2F*). The direct interaction between ICP34.5 and HSF1 was also identified by Co-IP assay. Importantly, HSF1 was effectively dephosphorylated at Ser320 as a result of the overexpression of ICP34.5, while no influence on the level of HSF1 expression was observed (*Figure 2G-H, Figure S7*). Considering that protein phosphatase 1 (PP1) can interact with ICP34.5 and dephosphorylate eIF2α (Li et al., 2011), we then investigated the interaction between PP1α and ICP34.5 (*Figure 2I*). Additionally, a direct interaction between PP1α and HSF1 was found, allowing for the dephosphorylation of HSF1 and then affecting its ability to reactivate HIV latency (*Figure 2J-L*). Collectively, these findings demonstrated that our modified

HSV-ΔICP34.5-based constructs effectively reactivated HIV latency by modulating the IKKα/β-NF-κB pathway and PP1-HSF1 pathway.

Recombinant HSV-ΔICP34.5 constructs expressing SIV antigens elicited robust immune responses in mice

Subsequently, we explored the potential of HSV-ΔICP34.5 as a bifunctional therapeutic vector to not only reactivate latent viral reservoirs but also induce antigen-specific immune responses against viral replication. To achieve this, SIV antigen genes were introduced into HSV-ΔICP34.5 vector based on BAC/ galK system. Additionally, the ICP47 gene was ablated to augment the immunogenicity of the HSV vector (*Figure 3A, Figure S8*). A series of recombinant HSV-ΔICP34.5ΔICP47-based vectors expressing SIV gag and env antigen were constructed, and the antigen expression of these constructs was confirmed by Western blotting assay (*Figure 3B-C*). Furthermore, to improve the immunogenicity of the targeted antigen, we fused the SIV gag with soluble PD1 (sPD1), enabling it to competitively bind with PD-L1 and thereby block the PD1/PD-L1 immune inhibitory pathway (*Figure 3D*). Consistent with the above findings, these HSV-ΔICP34.5ΔICP47-based SIV vaccines also efficiently reactivated HIV latency (*Figure S9*). Then, the immunogenicity of the above modified HSV-ΔICP34.5ΔICP47-based SIV vaccine was assessed in mice (*Figure 3E*). Our results showed that these constructs effectively elicited SIV antigen-specific T cell immune responses using the interferon γ (IFN-γ) ELISpot assay and the intracellular cytokine staining (ICS) assay. Of note, the frequency of SIV Gag-

specific IFN-γ -secreting spot-forming cells (SFCs) in the HSV-sPD1-SIVgag group (1350 SFCs per 10^6 splenocytes) was significantly higher than that in the HSV-SIVgag group (498 SFCs per 10^6 splenocytes) (*Figure 3F*). The frequency of SIV Env2-specific IFN-γ -secreting SFCs in the HSV- SIVenv group was significantly higher than the HSV-empty group (*Figure 3G*). Furthermore, the polyfunctionality of antigen-specific T cell subsets in response to SIV antigen stimulation was confirmed using the ICS assay (*Figure 3H-M*). Consistently, the HSV-sPD1-SIVgag group showed a significantly higher frequency of SIV-specific $CD3^+$ T, $CD4^+$ T, and $CD8^+$ T cell subsets secreting IFN-γ, IL-2, and TNF-α cytokines compared to the HSV-SIVgag group (*Figure 3I-K*). Notably, a heightened proportion of Gag-specific effector memory T cells (Tem) of $CD8^+$ T cell subset in HSV-ΔICP34.5ΔICP47-sPD1-SIVgag group was observed in comparison to the HSV-Gag group (*Figure 3L*). In addition, a higher frequency of SIV- Env2-specific $CD4^+$ T cells secreting IFN-γ was observed in the HSV-ΔICP34.5ΔICP47-SIVenv group than in the HSV-ΔICP34.5ΔICP47-empty group (*Figure 3M*). These data indicated that the vaccines constructed in this study elicited a robust T cell immune response in mice. Moreover, the blockade of PD1/PDL1 signaling pathway effectively enhanced vaccine-induced T cell immune responses, which was consistent with our and other previous studies (Zhou et al., 2013, Wu et al., 2022, Pan et al., 2018, Xiao et al., 2014).

The modified HSV-based constructs efficiently elicited SIV-specific immune responses in chronically SIV-infected macaques

Next, the immunogenicity of these HSV-ΔICP34.5ΔICP47-vectored SIV vaccines was further investigated in chronically SIV_{mac239}-infected rhesus macaques (RMs). To mimic chronically infected HIV patients in clinic practice, all RMs used in this study were chronically infected with SIV and received ART treatment for several years, as reported in our previous studies (Pan et al., 2018, Yang et al., 2019, Wu et al., 2021, Wu et al., 2022, He et al., 2023). Based on sex, age, viral load, and CD4 count, nine RMs were assigned into three groups: ART+saline group (n=3), ART+HSV-ΔICP34.5ΔICP47-empty group (n=3), and ART+HSV-ΔICP34.5ΔICP47-sPD1-SIVgag/SIVenv group (n=3) (*Table S2)*. All RMs received ART (FTC/6.7 mg/kg/once daily, PMPA/10 mg/kg/once daily) treatment to avoid the interference of free SIV particles. On day 33 and day 52, these RMs were immunized with saline, HSV-ΔICP34.5ΔICP47-empty, or HSV-ΔICP34.5ΔICP47-sPD1-SIVgag/SIVenv respectively. On day 70, ART treatment in all RMs was discontinued to evaluate the time interval of viral rebound. Samples were collected at different time points to monitor virological and immunological parameters (Figure 4A). To reduce the impact of individual RM variations, the difference in SIV-specific IFN-γ-secreting SFCs between post-immunization and pre-immunization (ΔSFCs) was used to evaluate the immune response induced by HSV-ΔICP34.5ΔICP47-vectored SIV vaccines. The results showed that SIV Gag-specific ΔSFCs in the ART+HSV-ΔICP34.5ΔICP47-sPD1-SIVgag/SIVenv group were greatly increased when compared with those in the ART+HSV-ΔICP34.5ΔICP47-empty group and ART+saline group (*Figure 4B-D*). A similar enhancement of SIV Gag-specific TNF-

α -secreting $CD4^+$ T and $CD8^+$ T subsets was also verified by ICS assay (*Figure 4E*). Collectively, these data demonstrated that the HSV-ΔICP34.5ΔICP47-sPD1-SIVgag/SIVenv construct elicited robust SIV-specific T cell immune responses in ART-treated, SIV-infected RMs.

The modified HSV-based constructs partly reactivated SIV latency *in vivo* and delayed viral rebound in chronically SIV-infected, ART-treated macaques

Finally, we investigated the therapeutic efficacy of HSV-ΔICP34.5ΔICP47-sPD1-SIVgag/SIVenv in chronically SIV-infected, ART-treated RMs. Consistent with our previous studies, the plasma viral load (VL) in these RMs was effectively suppressed during ART treatment, but rebounded after ART discontinuation. The VL in the ART+saline group promptly rebounded after ART discontinuation, and one of three RMs showed a sigficantly increased peak VL compared with the pre-ART VL (Figure 5A and 5D). However, plasma VL in the ART+HSV-ΔICP34.5ΔICP47-empty group and the ART+HSV-ΔICP34.5ΔICP47-sPD1-SIVgag/SIVenv group exhibited a delayed rebound interval (*Figure 5B-C*). Remarkably, there was a lower rebounded peak VL (two of three RMs) than pre-ART VL in the ART+HSV-ΔICP34.5ΔICP47-sPD1-SIVgag/SIVenv group, while two of three RMs had a higher rebounded peak VL than pre-ART VL in the ART+HSV-ΔICP34.5ΔICP47-empty group (*Figure 5D*). Then, we assessed the potential effect on the latent SIV reservoirs *in vivo* by administering our modified HSV-based SIV therapeutic constructs in these RMs. Although there were no

obvious viral blips observed in these RMs, we found significant suppression of total SIV DNA and integrated SIV DNA provirus in the ART+HSV-ΔICP34.5ΔICP47-sPD1-SIVgag/SIVenv group. However, the copies of the SIV DNA provirus were significantly improved in the ART+HSV-ΔICP34.5ΔICP47-empty group and ART+saline group (*Figure 5E-F*). More interestingly, we assessed the magnitude of SIV Pol antigen-specific immune responses, which could represent to some extent the level of newly generated virions from the reactivated SIV reservoirs, because SIV Pol antigen was not included in our designed vaccine constructs. Specifically, the Pol-specific SFCs amount on Day 70 (511 SFCs/10^6 PBMCs, post-vaccination) was higher than that on Day 33 (315 SFCs/10^6 PBMCs, pre-vaccination) in the ART+HSV-ΔICP34.5ΔICP47-sPD1-SIVgag/SIVenv group. In addition, there was a similar observation in the ART+HSV-ΔICP34.5ΔICP47-empty group. In contrast, the Pol-specific SFCs gradually decreased with the duration of ART treatment in the ART+saline group (*Figure 5G*). In addition, the $CD4^+$ /$CD8^+$ T cell ratio (*Figure 5H*) and body weight (*Figure S10*) after treatment were effectively ameliorated in the RMs of the ART+HSV-ΔICP34.5ΔICP47-sPD1-SIVgag/SIVenv group, but not in the ART+HSV-ΔICP34.5ΔICP47-empty group and ART+saline group. Our data also demonstrated that there was no significant effect on the cell composition of peripheral blood in the macaques of ART+HSV-ΔICP34.5ΔICP47-sPD1-SIVgag/SIVenv group (Figure S11). Taken together, these findings suggested that the latent SIV reservoirs might be effectively purged because of the effect of simultaneously reactivating viral latency and eliciting SIV-specific immune responses by our modified HSV-based SIV therapeutic constructs,

thus resulting in a delayed viral rebound in chronically SIV-infected, ART-treated macaques.

Discussion

To conquer the continuous epidemic of AIDS, exploring novel strategies to render and eliminate HIV latency should stand as a pivotal pursuit. Currently, numerous strategies, including shock and kill, block and lock, chimeric antigen receptor T-cell therapy, therapeutic vaccination, and gene editing, have been extensively investigated to target the latent HIV reservoirs for an HIV functional cure (Deeks, 2012, Yeh and Ho, 2021, Maldini et al., 2020, Herzig et al., 2019, Dash et al., 2023, Dashti et al., 2023, Walker-Sperling et al., 2022). However, there is no safe and effective approach for clinical use in HIV patients yet. In the present study, we occasionally found that the modified HSV-ΔICP34.5-based constructs could reactivate HIV latency more efficiently than wild-type HSV counterpart, which inspired us to develop a proof-of-concept strategy based on a bifunctional HSV-vectored therapeutic vaccine, aiming to simultaneously reactivate viral latency and elicit HIV/SIV-specific immune responses for HIV functional cure. Our results indicated that these modified HSV-based constructs efficiently elicited antigen-specific immune responses in mice and chronically SIV-infected macaques, and further therapeutic efficacy experiments showed that this strategy partly reactivated SIV latency *in vivo* and delayed viral rebound in chronically SIV-infected, ART-treated macaques (*Figure 6*).

The latent HIV proviruses can harbor it into the host genome with a quiescent transcription state, and thus cannot be recognized by immune surveillance or drug

311 killing (Churchill et al., 2016, Pierson et al., 2000). Therefore, it is critical to disrupt
312 viral latency for developing an HIV cure strategy. Based on our experimental data,
313 the mechanism for efficiently reactivating viral latency by the modified HSV-
314 ΔICP34.5-based constructs may involve regulating the IKKα/β-NF-κB pathway and
315 PP1-HSF1 pathway. Indeed, during its replication, HSV can activate the double-
316 stranded RNA-dependent protein kinase (PKR) pathway, and thus phosphorylate
317 the protein translation initiation regulator eIF2α, resulting in the initiation of protein
318 translation (Farassati et al., 2001). Previous studies have shown that the
319 reactivation potential of HSV might be intertwined with NF-κB, Sp1, and other
320 unknown transcription factors by ICP0, ICP4, and ICP27 (Chapman et al., 1991,
321 Amici et al., 2004, Vlach and Pitha, 1992, Mosca et al., 1987b, Golden et al., 1992,
322 Vlach and Pitha, 1993, Mosca et al., 1987a). However, the underlying mechanism
323 by which the ICP34.5-deleted HSV construct can greatly improve the reactivation
324 efficacy of HIV latency remains elusive.
325 ICP34.5 is a neurotoxicity factor that can antagonize innate immune responses,
326 including PKR, TANK binding kinase (TBK1) signaling, and Beclin1-mediated
327 apoptosis (He et al., 1997, Manivanh et al., 2017, Orvedahl et al., 2007). Thus,
328 ICP34.5 deletion is benificial to improve the safety of HSV-based constructs. As
329 expected, our data have demonstrated experimentally that HSV-ΔICP34.5
330 exhibited lower virulence and replication ability than wild-type HSV-1 (Figure S1).
331 Importantly, we also observed a significant decrease in the expression of
332 inflammatory factors in PWLH when compared to wild-type HSV-1 (Figure 1I-K).
333 These data suggested that the safety of HSV-ΔICP34.5 should be more tolerable

than wild-type HSV-1. ICP34.5 binds to host PP1 and mediates the dephosphorylation of eIF2α, thus allowing protein synthesis and reversing the effects of PKR and host antiviral functions (He et al., 1997, He et al., 1998). In this study, our findings further unveiled an interaction between ICP34.5 and HSF1, resulting in reduced HSF1 phosphorylation via recruitment of PP1α. Interestingly, previous reports indicated that HSF1 could positively regulate HIV gene transcription (Rawat and Mitra, 2011), which is facilitated by its nuclear entry post-phosphorylation and subsequent recruitment of p300 for self-acetylation, along with binding to the HIV-1 LTR. Studies have also shown that HSF1 could further orchestrate p-TEFb recruitment to promote HIV-1 transcriptional elongation (Peng et al., 2020, Lin et al., 2018, Pan et al., 2016b, Pan et al., 2016a). Under stress-induced conditions, phosphorylation triggers the formation of the HSF1 trimer, thus facilitating its nuclear entry to bind to heat shock elements (HSEs) for gene transcription regulation (Bonner et al., 2000, Timmons et al., 2020). Additionally, we also demonstrated that ICP34.5 interacted with IKKα and IKKβ, thereby impeding NF-κB nuclear entry and further curbing HIV latency. Consistently, previous studies have also suggested that ICP34.5 could disrupt the NF-κB pathway and possibly affect the maturation of dendritic cells (Jin et al., 2011). Intriguingly, these findings collectively indicated that ICP34.5 might plays an antagonistic role in the reactivation of HIV by HSV-1, and thus our modified HSV-ΔICP34.5 constructs can effectively reactivate HIV/SIV latency through the release of imprisonment from ICP34.5. However, ICP34.5 overexpression had only a partial effect on the reduction of the HIV latency reactivation, indicating that HSV-

ΔICP34.5-based constructs can also reactivate HIV latency through other yet-to-be-determined mechanisms.

Another observation in this study is that the HSV-ΔICP34.5ΔICP47-sPD1-SIVgag/SIVenv construct elicited robust and persistent SIV-specific T cell immune responses in ART-treated, chronically SIV-infected macaques. Increasing evidence has indicated that HIV-specific cytolytic T lymphocytes (CTLs) can facilitate the suppression of latent viral reservoirs, and thus, the induction of robust and persistent HIV-specific CTL responses is essential for achieving long-term disease-free and transmission-free HIV control (Collins et al., 2020). Featured polyfunctional $CD8^+$ T cells may contribute to HIV elite controllers or long-term non-progressors, a rare proportion of HIV-infected individuals who can spontaneously control viral replication even without ART treatment (Owen et al., 2010, Ferre et al., 2009, O'Connell et al., 2009). In addition, both our previous study and others have demonstrated that strong antigen-specific $CD8^+$ T cell immune responses, especially effector memory $CD8^+$ T cells, were associated with a lower viral load, and *in vivo* $CD8^+$ lymphocyte depletion with intravenous infusion of anti-CD8 monoclonal antibody could lead to dramatical viral rebound in these vaccinated elite macaques (Perdomo-Celis et al., 2022, Pandrea et al., 2011, Sun et al., 2013, Sun et al., 2010, Pan et al., 2018, Sun et al., 2012). Notably, previous studies have shown that HSV-based vaccines expressing HIV/SIV antigen did elicit specific $CD8^+$ T cell immune responses in mice and macaques, but the magnitude was not as strong as other viral vectors (Parker et al., 2007, Murphy et al., 2000, Kaur et al., 2007). Therefore, to further improve its immunogenicity *in vivo*, some

modifications were adopted to optimize the HSV-vectored vaccine. 1) The ICP47 protein, encoded by the US12 gene, can bind to the transporter associated with antigen presentation (TAP) 1/2, inhibiting the transport of viral peptides into the endoplasmic reticulum and the loading of peptides onto nascent major histocompatibility complex (MHC) class I molecules to activate $CD8^+$ T cells (Orr et al., 2005). Therefore, the ICP47 gene was deleted from our developed HSV vector. 2) Negatively immunoregulatory molecules, including PD1, TIM-3, and LAG-3, are usually involved in the pathogenesis of HIV infection, as well as in chronically SIV-infected macaques. Among them, PD1 upregulation can result in the exhaustion and dysfunction of $CD8^+$ T cells (Trautmann et al., 2006). In addition, PD1 expression on memory $CD4^+$ T cells might be linked with HIV latency. In this study, we modified the SIV antigen by fusing to soluble PD1 (sPD1), which can block the PD1/PDL1 pathway by competitively binding with PDL1 and thus improve HIV/SIV vaccine-induced $CD8^+$ T cell immune responses (Zhou et al., 2013, Wu et al., 2022, Pan et al., 2018, Xiao et al., 2014).

Although promising, there are still some limitations to our study. Firstly, this is a pilot study with a relatively small numbers of RMs, and future studies with a larger number of animals can be conducted to better verify our strategy. Secondly, the HSV-ΔICP34.5ΔICP47-sPD1-SIVgag/SIVenv vaccine resulted in delayed viral rebound and a lower peak viral load post-rebound than pre-ART treatment but did not completely suppress SIV virus rebound in this study, which may be attributed to suboptimal doses and treatment, implying that we should further optimize this regimen for eventually achieving an HIV functional cure in future studies. The

current consensus on HIV/AIDS vaccines emphasizes the importance of simultaneously inducing broadly neutralizing antibodies and cellular immune responses. Therefore, we believe that incorporating the induction of broadly neutralizing antibodies into our future optimizing approaches may lead to better therapeutic outcomes. Taken together, these findings demonstrated that our modified HSV-ΔICP34.5-based constructs potentially reactivated HIV/SIV latency by modulating the IKKα/β-NF-κB pathway and PP1-HSF1 pathway, and thereby we developed a proof-of-concept strategy based on a bifunctional HSV-vectored therapeutic vaccine, which can provide insights into the rational design of novel strategies for pursuing an HIV functional cure.

Methods

Mouse ethics statement and vaccination

Female BALB/c mice, aged six to eight weeks, were procured from the Experimental Animal Center of Sun Yat-sen University. A total of twenty-five mice were randomly divided into five groups to evaluate the immunogenicity of the recombinant HSV-vector-based SIV vaccine. During the initial week, each mouse was subcutaneously administered a vaccination of 1×10^6 PFU of the respective recombinant HSV-vector vaccines (HSV-ΔICP34.5ΔICP47-empty, HSV-ΔICP34.5ΔICP47-sPD1, HSV-ΔICP34.5ΔICP47-SIVgag, HSV-ΔICP34.5ΔICP47-sPD1-SIVgag, HSV-ΔICP34.5ΔICP47-SIVenv). Following a two-week interval, a booster vaccination was administered via the subcutaneous route using 2×10^6 PFU of recombinant HSV-vector vaccines. The subsequent assessment of the

immune response involved ELISpot and intracellular cytokine staining (ICS) assays in accordance with the vaccination schedule.

Ethics statement and vaccination of macaques

A total of 9 chronically SIV_{mac239}-infected rhesus macaques (RMs) were included in this study. All RMs received ART treatment (FTC/6.7 mg/kg/once daily, PMPA/10 mg/kg/once daily) for a duration of 33 days. The RMs were allocated into three groups based on their baseline plasma SIV viral loads (VL): ART + saline (n=3) as the control group, ART+ HSV-ΔICP34.5ΔICP47-empty (n=3) as the sham group, and ART+ HSV-ΔICP34.5ΔICP47-sPD1-SIVgag/SIVenv (n=3) as the vaccinated group. On day 0, all RMs received ART treatment. Once the VL dropped below the limit of detection (1×10^2 copies/mL), the vaccinated group and sham group were primed with a subcutaneous vaccination of 1×10^7 PFU HSV-ΔICP34.5ΔICP47-sPD1-SIVgag/SIVenv or HSV-ΔICP34.5ΔICP47-empty, respectively, while the control group received an injection of 0.9% saline. After three weeks of the prime vaccination, the vaccinated group and sham group RMs received a subcutaneous booster vaccination of 5×10^7 PFU HSV-ΔICP34.5ΔICP47-sPD1-SIVgag/SIVenv or HSV-ΔICP34.5ΔICP47-empty, respectively. After two weeks of booster vaccination, the ART treatment for all RMs was interrupted. The immune response was evaluated by IFN-γ ELISpot and ICS assays. Plasma viral load was regularly monitored throughout the studied period.

Peptide pools

The peptide pools, encompassing the complete sequences of SIV Gag, Env, and Pol proteins, comprising 15 amino acids with 11 overlaps, were generously provided by the HIV Reagent Program, National Institutes of Health (NIH), USA. Gag pools comprise 125 peptides, while Env and Pol pools are subdivided into Env1 (109 peptides) and Env2 (109 peptides) pools, as well as Pol1 (131 peptides) and Pol2 (132 peptides) pools. These peptide pools were dissolved in dimethyl sulfoxide (DMSO, Sigma) at a concentration of 0.4 mg/ peptide/mL for subsequent immunological assays.

Construction of recombinant HSV

For the generation of recombinant HSV-vector-based vaccines, we implemented modifications at the ICP34.5 loci through homologous recombination within the BAC-HSV-1 system. Specifically, double copies of the ICP34.5 and ICP47 genes were either deleted or inserted into the respective counterparts: sPD1, SIVgag, sPD1-SIVgag, and SIVenv genes. The sPD1-SIVgag gene was created by fusing the N-terminal region of mouse soluble PD1 (sPD1) with the C-terminal segment of SIVgag, connected by a GGGSGGG linker, which was engineered through overlapping PCR.

Plaque Assay

Vero cells were seeded at a density of 2×10^5 cells per well in a 12-well plate and cultured for 24 h. Virus samples were serially diluted and then added to the wells. After 2 h of incubation at 37°C with 5% CO_2, the supernatant was aspirated, and the cells were washed with PBS. Then, a medium containing 1% FBS, 1% low-melting-point agarose, and 1% penicillin-streptomycin was added to each well.

After 3 days of incubation, cells were fixed with 4% paraformaldehyde at room temperature for 2 h and stained with 1% crystal violet for 10 min. Plaques were visualized and counted, and virus titers were calculated as plaque-forming units per milliliter (PFU/mL).

IFN-γ ELISpot assay

The IFN-γ- ELISpot assay was conducted in accordance with our previous study (Sun et al., 2010). In the mouse experiment, 2.5×10^5 freshly isolated mouse spleen lymphocytes were simulated with SIV Gag, Env1, and Env2 peptide pools. In the monkey experiment, 2×10^5 peripheral blood mononuclear cells (PBMCs) were seeded and simulated with the SIV Gag, Env, and Pol peptide pools. DMSO (Sigma) was utilized as Mock stimulation, while concanavalin A (ConA, 10 μg/mL) was employed as a positive control. Spot quantification was performed using an ELISpot reader (Mabtech), and peptide-specific spot counts were determined by subtracting the spots from mock stimulation.

Intracellular cytokine staining (ICS)

The ICS assay was performed as described previously (Wu et al., 2022). In the mouse experiment, 2×10^6 freshly isolated mouse spleen lymphocytes were stimulated with SIV Gag, Env1, and Env2 peptide pools. For the monkey experiment, 2×10^6 PBMCs were seeded and simulated with the SIV Gag, Env, and Pol peptide pools. DMSO and PMA (Thermo Scientific) plus ionomycin were used as the mock and positive controls, respectively. Data analysis was performed using FlowJo software (version 10.8.1), and the antibodies used are listed in *Table S3*.

The frequencies of cytokines produced from peptide-specific cells were analyzed by subtracting mock stimulation.

SIV viral RNA and DNA copy assays and absolute T cell count

Absolute T cell count and the levels of plasma mRNA and SIV total DNA were quantified as described previously (Wu et al., 2022). Plasma viral RNA copy numbers were determined via SYBR green-based real-time quantitative PCR (Takara), using SIV gag-specific primers (*Table S4*). Viral RNA copy numbers were calculated based on the standard curve established using SIV_{mac239} gag standards. The lower limit of detection for this assay was 100 copies/mL of plasma. Total cellular DNA was extracted from approximately 0.5 to 5 million cells using a QIAamp DNA Blood Minikit (Qiagen). PCR assays were performed with 200 ng samples of DNA, and SIV viral DNA was quantified using a pair of primers targeting a conserved region of the SIV gag gene, as previously described. Quantitation was performed by comparing the results to the standard curve of SIV gag copies. Integrated SIVmac239 DNA was measured using nested PCR with two sets of primers. The first round used SIVgag-reverse and Alu-forward primers, while the second round used primers specific to a conserved SIVgag region. Quantification was compared to a standard of CEMss/pWPXLD-rc cell genome as our previously described (Yang et al., 2019).

Plasmids, cells, and viruses

pVAX-Myc-PDL1, pVAX-Flag-ICP34.5, pVAX-Myc-HSF1, pVAX-HA-PP1α: full-length mouse PDL1, full-length HSV-1 ICP34.5, and full-length human HSF1 and human PP1α with N or C-terminal Tag were cloned into the pVAX vector. pVAX-

empty, pcDNA3.1-IKKα, and pcDNA3.1-IKKβ plasmids were stored in our laboratory. pVAX-empty was used as a mock transfection in our study.

293T cells (from the embryonic kidney of a female human fetus), Vero cells (from the kidney of a female normal adult African green monkey), and Hela cells (from the cervical cancer cells of an African American woman) were cultured in complete Dulbecco's modified Eagle's medium (DMEM, Gibco) containing 10% fetal bovine serum (FBS, Gibco) and 1% penicillin/streptomycin (Gibco) at 37°C in an atmosphere of 5% CO_2. The J-Lat 10.6 cells (Jurkat cells contain the HIV-1 full-length genome whose Env was frameshifted and inserted with GFP in place of Nef) and the HIV-1 latently infected $CD4^+$ CEM cells ACH-2 (A3.01 cell integrated HIV-1 proviral DNA) were cultured in complete RPIM640 (Gibco) containing 10% FBS and 1% penicillin/streptomycin at 37°C in an atmosphere of 5% CO_2. J-Lat 10.6-ICP34.5 cells were constructed in our laboratory.

The HSV-1 (McKrae) strains were stored in our laboratory. HSV-GFP (17 strain) was rescued from pBAC-GFP-HSV in Vero cells. HSV-ΔICP34.5 (17 strain) was rescued from pBAC-GFP-HSV-ΔICP34.5 (with deletion of double copies of ICP34.5 gene) in Vero cells.

RT-qPCR

RT-qPCR was performed as described in our previous study (Zhao et al., 2022). Data were normalized to β-actin. The primer sequences are listed in Supplemental *Table 4*. Fold changes in the threshold cycle (Ct) values were calculated using the $2^{-\Delta\Delta Ct}$ method.

Chromatin immunoprecipitation (ChIP) assay

ChIP analysis was conducted using the SimpleChIP Enzymatic Chromatin IP kit (Agarose Beads) (CST), following the manufacturer's instructions. Quantitative real-time PCR was employed for detecting the LTR sequence. The sequences of primers used in the LTR ChIP are listed in Supplemental Table 4. % Input= 2% × $2^{[(ct)2\% \text{ input sample (ct) IP sample}]}$.

Co-immunoprecipitation (Co-IP)

Cells were harvested and subjected to Co-IP assay, following the protocol outlined in our previous study (Zhao et al., 2022).

Protein extraction and western blot

Nuclear and cytoplasmic proteins were extracted by kits following the manufacturer's instructions (Beyotime). The Western blotting assay was performed as previously described (Zhao et al., 2022).

Statistical analysis

GraphPad Prism 8.0 (GraphPad Software, San Diego, California) was used for statistical analysis. For intragroup direct comparisons, Student's unpaired two-tailed *t* test was performed to analyze significant differences. For comparisons of multiple groups, one-way ANOVAs were performed. Significance levels are indicated as *P< 0.05, ** P< 0.01, *** P< 0.001, **** P< 0.0001.

Study approval

Mice experiment was approved by the Laboratory Animal Ethics Committee guidelines at Sun Yat-sen University (approval number: SYSU-IACUC-2021-000185). Chinese rhesus macaques (Macaca mulatta) were housed at the Landau

Animal Experimental Center, Guangdong Landau Biotechnology Co., Ltd. (approval number: N2021101). The primary PBMC samples were isolated from the chronically HIV-1-infected participants who were recruited from Guangzhou Eighth People's Hospital (Guangzhou, Guangdong, China), which was approved by the Medical Ethics Review Board of the School of Public Health (Shenzhen), Sun Yat-sen University (2022-037). All participants provided written informed consent, agreeing to participate in this study. The enrollment criteria for HIV-1-infected individuals included substained suppression of plasma HIV-1 viremia under ART, with undetectable plasma HIV-1 RNA levels (less than 50 copies/mL) for at least 12 months and a $CD4^+$ T cell count more than 350 cells/μL).

Acknowledgements

We appreciate the staff at the Animal Center of GIBH for their excellent technical assistance. We thank all other members of our group for their helpful advice and discussion to improve this project. We also appreciate the NIH AIDS Research and Reference Reagent Program for providing SIV peptide pools.

Additional information

Competing interests

The authors have declared that no conflict of interest exists.

Funding

This project was supported by National Natural Science Foundation of China (82271786, 81971927, 32370171), Science and Technology Planning Project of Guangdong Province, China (2021B1212040017), Shenzhen Key Laboratory of Pathogenic Microbes and Biosafety (ZDSYS20230626091203007), the Sanming

Project of Medicine in Shenzhen Nanshan (SZSM202103008), and the Key Subject of Nanshan district of Shenzhen for AIDS surveillance and prevention.

Author Contributions

All authors were involved in drafting or critically revising the manuscript for important intellectual content, and all authors approved the final version for publication. CS conceived the project and provided the main funding. CS and LC designed the experiments and reviewed the manuscript. ZW, PL, YY, and CW performed most of the experiments and analyzed the data. ZW, PL, YY, CW, ML, HW, MS, YH, and MC established the animal models and performed animal experiments. ZW and CS interpreted the data and wrote the manuscript.

Additional files

Supplementary files

Figure S1-S11. Table S1-S4.

Data Availability Statement

Source data contain the numerical data used to generate the figures.

References

AMICI, C., BELARDO, G., ROSSI, A. & SANTORO, M. G. 2001. Activation of I kappa b kinase by herpes simplex virus type 1. A novel target for anti-herpetic therapy. ***J Biol Chem* 276**: 28759.DOI: https://doi.org/10.1074/jbc.M103408200, PMID: 11387335

AMICI, C., BELARDO, G., ROZERA, C., BERNASCONI, D. & SANTORO, M. G. 2004. Inhibition of herpesvirus-induced HIV-1 replication by cyclopentenone prostaglandins: role of IkappaB kinase (IKK). ***Aids* 18**: 1271.DOI: https://doi.org/10.1097/00002030-200406180-00005, PMID: 15362659

ARCHIN, N. M., KIRCHHERR, J. L., SUNG, J. A., CLUTTON, G., SHOLTIS, K., XU, Y., ALLARD, B., STUELKE, E., KASHUBA, A. D., KURUC, J. D., ERON, J., GAY, C. L., GOONETILLEKE, N. & MARGOLIS, D. M. 2017. Interval dosing with the HDAC inhibitor vorinostat effectively reverses HIV latency. ***J Clin Invest* 127**: 3126.DOI: https://doi.org/10.1172/jci92684, PMID: 28714868

ARCHIN, N. M., SUNG, J. M., GARRIDO, C., SORIANO-SARABIA, N. & MARGOLIS, D. M. 2014. Eradicating HIV-1 infection: seeking to clear a persistent pathogen. ***Nat Rev Microbiol* 12**: 750.DOI: https://doi.org/10.1038/nrmicro3352, PMID: 25402363

614 BISGROVE, D. A., MAHMOUDI, T., HENKLEIN, P. & VERDIN, E. 2007. Conserved P-TEFb-
615 interacting domain of BRD4 inhibits HIV transcription. ***Proc Natl Acad Sci U S A* 104**:
616 13690.DOI: https://doi.org/10.1073/pnas.0705053104, PMID: 17690245
617 BONNER, J. J., CHEN, D., STOREY, K., TUSHAN, M. & LEA, K. 2000. Structural analysis of yeast
618 HSF by site-specific crosslinking. ***J Mol Biol* 302**: 581.DOI:
619 https://doi.org/10.1006/jmbi.2000.4096, PMID: 10986120
620 CALISTRI, A., PAROLIN, C. & PALù, G. 2003. Herpes simplex virus type 1 can either suppress or
621 enhance human immunodeficiency virus type 1 replication in CD4-positive T lymphocytes.
622 ***J Med Virol* 70**: 163.DOI: https://doi.org/10.1002/jmv.10350, PMID: 12629659
623 CHAPMAN, C. J., HARRIS, J. D., COLLINS, M. K. L. & LATCHMAN, D. S. 1991. A recombinant
624 HIV provirus is synergistically activated by the HIV Tat protein and the HSV IE1 protein but
625 not by the HSV IE3 protein. ***AIDS* 5**,
626 CHURCHILL, M. J., DEEKS, S. G., MARGOLIS, D. M., SILICIANO, R. F. & SWANSTROM, R. 2016.
627 HIV reservoirs: what, where and how to target them. ***Nat Rev Microbiol* 14**: 55.DOI:
628 https://doi.org/10.1038/nrmicro.2015.5, PMID: 26616417
629 COLLINS, D. R., GAIHA, G. D. & WALKER, B. D. 2020. CD8(+) T cells in HIV control, cure and
630 prevention. ***Nat Rev Immunol* 20**: 471.DOI: https://doi.org/10.1038/s41577-020-0274-9,
631 PMID: 32051540
632 DASH, P. K., CHEN, C., KAMINSKI, R., SU, H., MANCUSO, P., SILLMAN, B., ZHANG, C., LIAO,
633 S., SRAVANAM, S., LIU, H., WAIGHT, E., GUO, L., MATHEWS, S., SARIYER, R., MOSLEY,
634 R. L., POLUEKTOVA, L. Y., CAOCCI, M., AMINI, S., GORANTLA, S., BURDO, T. H.,
635 EDAGWA, B., GENDELMAN, H. E. & KHALILI, K. 2023. CRISPR editing of CCR5 and HIV-
636 1 facilitates viral elimination in antiretroviral drug-suppressed virus-infected humanized
637 mice. ***Proc Natl Acad Sci U S A* 120**: e2217887120.DOI:
638 https://doi.org/10.1073/pnas.2217887120, PMID: 37126704
639 DASHTI, A., SUKKESTAD, S., HORNER, A. M., NEJA, M., SIDDIQI, Z., WALLER, C., GOLDY, J.,
640 MONROE, D., LIN, A., SCHOOF, N., SINGH, V., MAVIGNER, M., LIFSON, J. D.,
641 DELEAGE, C., TUYISHIME, M., FALCINELLI, S. D., KING, H. A. D., KE, R., MASON, R.
642 D., ARCHIN, N. M., DUNHAM, R. M., SAFRIT, J. T., JEAN, S., PERELSON, A. S.,
643 MARGOLIS, D. M., FERRARI, G., ROEDERER, M., SILVESTRI, G. & CHAHROUDI, A.
644 2023. AZD5582 plus SIV-specific antibodies reduce lymph node viral reservoirs in
645 antiretroviral therapy-suppressed macaques. ***Nat Med***.DOI:
646 https://doi.org/10.1038/s41591-023-02570-7, PMID: 37783968
647 DEEKS, S. G. 2012. HIV: Shock and kill. ***Nature* 487**: 439.DOI: https://doi.org/10.1038/487439a,
648 PMID: 22836995
649 FARASSATI, F., YANG, A. D. & LEE, P. W. 2001. Oncogenes in Ras signalling pathway dictate
650 host-cell permissiveness to herpes simplex virus 1. ***Nat Cell Biol* 3**: 745.DOI:
651 https://doi.org/10.1038/35087061, PMID: 11483960
652 FERRE, A. L., HUNT, P. W., CRITCHFIELD, J. W., YOUNG, D. H., MORRIS, M. M., GARCIA, J.
653 C., POLLARD, R. B., YEE, H. F., JR., MARTIN, J. N., DEEKS, S. G. & SHACKLETT, B. L.
654 2009. Mucosal immune responses to HIV-1 in elite controllers: a potential correlate of
655 immune control. ***Blood* 113**: 3978.DOI: https://doi.org/10.1182/blood-2008-10-182709,
656 PMID: 19109229
657 GOLDEN, M. P., KIM, S., HAMMER, S. M., LADD, E. A., SCHAFFER, P. A., DELUCA, N. &
658 ALBRECHT, M. A. 1992. Activation of human immunodeficiency virus by herpes simplex
659 virus. ***J Infect Dis* 166**: 494.DOI: https://doi.org/10.1093/infdis/166.3.494, PMID: 1354237
660 HE, B., GROSS, M. & ROIZMAN, B. 1998. The gamma134.5 protein of herpes simplex virus 1 has
661 the structural and functional attributes of a protein phosphatase 1 regulatory subunit and
662 is present in a high molecular weight complex with the enzyme in infected cells. ***J Biol***
663 ***Chem* 273**: 20737.DOI: https://doi.org/10.1074/jbc.273.33.20737, PMID: 9694816
664 HE, B., GROSS, M. & ROIZMAN, B. 1997. The gamma(1)34.5 protein of herpes simplex virus 1
665 complexes with protein phosphatase 1alpha to dephosphorylate the alpha subunit of the
666 eukaryotic translation initiation factor 2 and preclude the shutoff of protein synthesis by
667 double-stranded RNA-activated protein kinase. ***Proc Natl Acad Sci U S A* 94**: 843.DOI:
668 https://doi.org/10.1073/pnas.94.3.843, PMID: 9023344

669 HE, Y., WU, C., LIU, Z., ZHANG, Y., FENG, F., LIN, Z., WANG, C., YANG, Q., WEN, Z., LIU, Y.,
670 ZHANG, F., LIN, Y., ZHANG, H., QU, L., LI, L., CAI, W., SUN, C., CHEN, L. & LI, P. 2023.
671 Arsenic trioxide-induced apoptosis contributes to suppression of viral reservoir in SIV-
672 infected rhesus macaques. ***Microbiol Spectr***: e0052523.DOI:
673 https://doi.org/10.1128/spectrum.00525-23, PMID: 37695104
674 HENG, M. C., HENG, S. Y. & ALLEN, S. G. 1994. Co-infection and synergy of human
675 immunodeficiency virus-1 and herpes simplex virus-1. ***Lancet* 343**: 255.DOI:
676 https://doi.org/10.1016/s0140-6736(94)91110-x, PMID: 7905094
677 HERZIG, E., KIM, K. C., PACKARD, T. A., VARDI, N., SCHWARZER, R., GRAMATICA, A., DEEKS,
678 S. G., WILLIAMS, S. R., LANDGRAF, K., KILLEEN, N., MARTIN, D. W., WEINBERGER,
679 L. S. & GREENE, W. C. 2019. Attacking Latent HIV with convertibleCAR-T Cells, a Highly
680 Adaptable Killing Platform. ***Cell* 179**: 880.DOI: https://doi.org/10.1016/j.cell.2019.10.002,
681 PMID: 31668804
682 JIN, H., YAN, Z., MA, Y., CAO, Y. & HE, B. 2011. A herpesvirus virulence factor inhibits dendritic
683 cell maturation through protein phosphatase 1 and Ikappa B kinase. ***J Virol* 85**: 3397.DOI:
684 https://doi.org/10.1128/jvi.02373-10, PMID: 21248029
685 KAUR, A., SANFORD, H. B., GARRY, D., LANG, S., KLUMPP, S. A., WATANABE, D., BRONSON,
686 R. T., LIFSON, J. D., ROSATI, M., PAVLAKIS, G. N., FELBER, B. K., KNIPE, D. M. &
687 DESROSIERS, R. C. 2007. Ability of herpes simplex virus vectors to boost immune
688 responses to DNA vectors and to protect against challenge by simian immunodeficiency
689 virus. ***Virology* 357**: 199.DOI: https://doi.org/10.1016/j.virol.2006.08.007, PMID:
690 16962628
691 KIM, Y., ANDERSON, J. L. & LEWIN, S. R. 2018. Getting the "Kill" into "Shock and Kill": Strategies
692 to Eliminate Latent HIV. ***Cell Host Microbe* 23**: 14.DOI:
693 https://doi.org/10.1016/j.chom.2017.12.004, PMID: 29324227
694 LEHRMAN, G., HOGUE, I. B., PALMER, S., JENNINGS, C., SPINA, C. A., WIEGAND, A., LANDAY,
695 A. L., COOMBS, R. W., RICHMAN, D. D., MELLORS, J. W., COFFIN, J. M., BOSCH, R. J.
696 & MARGOLIS, D. M. 2005. Depletion of latent HIV-1 infection in vivo: a proof-of-concept
697 study. ***Lancet* 366**: 549.DOI: https://doi.org/10.1016/s0140-6736(05)67098-5, PMID:
698 16099290
699 LEITMAN, E. M., THOBAKGALE, C. F., ADLAND, E., ANSARI, M. A., RAGHWANI, J.,
700 PRENDERGAST, A. J., TUDOR-WILLIAMS, G., KIEPIELA, P., HEMELAAR, J., BRENER,
701 J., TSAI, M. H., MORI, M., RIDDELL, L., LUZZI, G., JOOSTE, P., NDUNG'U, T., WALKER,
702 B. D., PYBUS, O. G., KELLAM, P., NARANBHAI, V., MATTHEWS, P. C., GALL, A. &
703 GOULDER, P. J. R. 2017. Role of HIV-specific CD8(+) T cells in pediatric HIV cure
704 strategies after widespread early viral escape. ***J Exp Med* 214**: 3239.DOI:
705 https://doi.org/10.1084/jem.20162123, PMID: 28983013
706 LI, Y., ZHANG, C., CHEN, X., YU, J., WANG, Y., YANG, Y., DU, M., JIN, H., MA, Y., HE, B. & CAO,
707 Y. 2011. ICP34.5 protein of herpes simplex virus facilitates the initiation of protein
708 translation by bridging eukaryotic initiation factor 2alpha (eIF2alpha) and protein
709 phosphatase 1. ***J Biol Chem* 286**: 24785.DOI: https://doi.org/10.1074/jbc.M111.232439,
710 PMID: 21622569
711 LI, Z., GUO, J., WU, Y. & ZHOU, Q. 2013. The BET bromodomain inhibitor JQ1 activates HIV
712 latency through antagonizing Brd4 inhibition of Tat-transactivation. ***Nucleic Acids Res* 41**:
713 277.DOI: https://doi.org/10.1093/nar/gks976, PMID: 23087374
714 LIN, J., ZHANG, X., LU, W., XU, X., PAN, X., LIANG, T., DUAN, S., CHEN, Y., LI, L. & LIU, S. 2018.
715 PR-957, a selective immunoproteasome inhibitor, reactivates latent HIV-1 through p-TEFb
716 activation mediated by HSF-1. ***Biochem Pharmacol* 156**: 511.DOI:
717 https://doi.org/10.1016/j.bcp.2018.08.042, PMID: 30170098
718 LOOKER, K. J., ELMES, J. A. R., GOTTLIEB, S. L., SCHIFFER, J. T., VICKERMAN, P., TURNER,
719 K. M. E. & BOILY, M. C. 2017. Effect of HSV-2 infection on subsequent HIV acquisition: an
720 updated systematic review and meta-analysis. ***Lancet Infect Dis* 17**: 1303.DOI:
721 https://doi.org/10.1016/s1473-3099(17)30405-x, PMID: 28843576
722 MALDINI, C. R., CLAIBORNE, D. T., OKAWA, K., CHEN, T., DOPKIN, D. L., SHAN, X., POWER,
723 K. A., TRIFONOVA, R. T., KRUPP, K., PHELPS, M., VRBANAC, V. D., TANNO, S.,

BATESON, T., LESLIE, G. J., HOXIE, J. A., BOUTWELL, C. L., RILEY, J. L. & ALLEN, T. M. 2020. Dual CD4-based CAR T cells with distinct costimulatory domains mitigate HIV pathogenesis in vivo. ***Nat Med* 26**: 1776.DOI: https://doi.org/10.1038/s41591-020-1039-5, PMID: 32868878

MANIVANH, R., MEHRBACH, J., KNIPE, D. M. & LEIB, D. A. 2017. Role of Herpes Simplex Virus 1 γ34.5 in the Regulation of IRF3 Signaling. ***J Virol* 91**.DOI: https://doi.org/10.1128/jvi.01156-17, PMID: 28904192

MOSCA, J. D., BEDNARIK, D. P., RAJ, N. B., ROSEN, C. A., SODROSKI, J. G., HASELTINE, W. A., HAYWARD, G. S. & PITHA, P. M. 1987a. Activation of human immunodeficiency virus by herpesvirus infection: identification of a region within the long terminal repeat that responds to a trans-acting factor encoded by herpes simplex virus 1. ***Proc Natl Acad Sci U S A* 84**: 7408.DOI: https://doi.org/10.1073/pnas.84.21.7408, PMID: 2823260

MOSCA, J. D., BEDNARIK, D. P., RAJ, N. B., ROSEN, C. A., SODROSKI, J. G., HASELTINE, W. A. & PITHA, P. M. 1987b. Herpes simplex virus type-1 can reactivate transcription of latent human immunodeficiency virus. ***Nature* 325**: 67.DOI: https://doi.org/10.1038/325067a0, PMID: 3025748

MURPHY, C. G., LUCAS, W. T., MEANS, R. E., CZAJAK, S., HALE, C. L., LIFSON, J. D., KAUR, A., JOHNSON, R. P., KNIPE, D. M. & DESROSIERS, R. C. 2000. Vaccine protection against simian immunodeficiency virus by recombinant strains of herpes simplex virus. ***J Virol* 74**: 7745.DOI: https://doi.org/10.1128/jvi.74.17.7745-7754.2000, PMID: 10933680

O'CONNELL, K. A., BAILEY, J. R. & BLANKSON, J. N. 2009. Elucidating the elite: mechanisms of control in HIV-1 infection. ***Trends Pharmacol Sci* 30**: 631.DOI: https://doi.org/10.1016/j.tips.2009.09.005, PMID: 19837464

ORR, M. T., EDELMANN, K. H., VIEIRA, J., COREY, L., RAULET, D. H. & WILSON, C. B. 2005. Inhibition of MHC class I is a virulence factor in herpes simplex virus infection of mice. ***PLoS Pathog* 1**: e7.DOI: https://doi.org/10.1371/journal.ppat.0010007, PMID: 16201019

ORVEDAHL, A., ALEXANDER, D., TALLóCZY, Z., SUN, Q., WEI, Y., ZHANG, W., BURNS, D., LEIB, D. A. & LEVINE, B. 2007. HSV-1 ICP34.5 confers neurovirulence by targeting the Beclin 1 autophagy protein. ***Cell Host Microbe* 1**: 23.DOI: https://doi.org/10.1016/j.chom.2006.12.001, PMID: 18005679

OWEN, R. E., HEITMAN, J. W., HIRSCHKORN, D. F., LANTERI, M. C., BISWAS, H. H., MARTIN, J. N., KRONE, M. R., DEEKS, S. G. & NORRIS, P. J. 2010. HIV+ elite controllers have low HIV-specific T-cell activation yet maintain strong, polyfunctional T-cell responses. ***Aids* 24**: 1095.DOI: https://doi.org/10.1097/QAD.0b013e3283377a1e, PMID: 20400885

PAN, E., FENG, F., LI, P., YANG, Q., MA, X., WU, C., ZHAO, J., YAN, H., CHEN, R., CHEN, L. & SUN, C. 2018. Immune Protection of SIV Challenge by PD-1 Blockade During Vaccination in Rhesus Monkeys. ***Front Immunol* 9**: 2415.DOI: https://doi.org/10.3389/fimmu.2018.02415, PMID: 30405615

PAN, X. Y., ZHAO, W., WANG, C. Y., LIN, J., ZENG, X. Y., REN, R. X., WANG, K., XUN, T. R., SHAI, Y. & LIU, S. W. 2016a. Heat Shock Protein 90 Facilitates Latent HIV Reactivation through Maintaining the Function of Positive Transcriptional Elongation Factor b (p-TEFb) under Proteasome Inhibition. ***J Biol Chem* 291**: 26177.DOI: https://doi.org/10.1074/jbc.M116.743906, PMID: 27799305

PAN, X. Y., ZHAO, W., ZENG, X. Y., LIN, J., LI, M. M., SHEN, X. T. & LIU, S. W. 2016b. Heat Shock Factor 1 Mediates Latent HIV Reactivation. ***Sci Rep* 6**: 26294.DOI: https://doi.org/10.1038/srep26294, PMID: 27189267

PANDREA, I., GAUFIN, T., GAUTAM, R., KRISTOFF, J., MANDELL, D., MONTEFIORI, D., KEELE, B. F., RIBEIRO, R. M., VEAZEY, R. S. & APETREI, C. 2011. Functional cure of SIVagm infection in rhesus macaques results in complete recovery of CD4+ T cells and is reverted by CD8+ cell depletion. ***PLoS Pathog* 7**: e1002170.DOI: https://doi.org/10.1371/journal.ppat.1002170, PMID: 21829366

PARKER, S. D., ROTTINGHAUS, S. T., ZAJAC, A. J., YUE, L., HUNTER, E., WHITLEY, R. J. & PARKER, J. N. 2007. HIV-1(89.6) Gag expressed from a replication competent HSV-1 vector elicits persistent cellular immune responses in mice. ***Vaccine* 25**: 6764.DOI: https://doi.org/10.1016/j.vaccine.2007.06.064, PMID: 17706843

PENG, W., HONG, Z., CHEN, X., GAO, H., DAI, Z., ZHAO, J., LIU, W., LI, D. & DENG, K. 2020. Thiostrepton Reactivates Latent HIV-1 through the p-TEFb and NF-κB Pathways Mediated by Heat Shock Response. ***Antimicrob Agents Chemother* 64**.DOI: https://doi.org/10.1128/aac.02328-19, PMID: 32094131

PERDOMO-CELIS, F., PASSAES, C., MONCEAUX, V., VOLANT, S., BOUFASSA, F., DE TRUCHIS, P., MARCOU, M., BOURDIC, K., WEISS, L., JUNG, C., BOURGEOIS, C., GOUJARD, C., MEYER, L., MüLLER-TRUTWIN, M., LAMBOTTE, O. & SáEZ-CIRIóN, A. 2022. Reprogramming dysfunctional CD8+ T cells to promote properties associated with natural HIV control. ***J Clin Invest* 132**.DOI: https://doi.org/10.1172/jci157549, PMID: 35380989

PIERCE, C. A., LOH, L. N., STEACH, H. R., CHESHENKO, N., PRESTON-HURLBURT, P., ZHANG, F., STRANSKY, S., KRAVETS, L., SIDOLI, S., PHILBRICK, W., NASSAR, M., KRISHNASWAMY, S., HEROLD, K. C. & HEROLD, B. C. 2023. HSV-2 triggers upregulation of MALAT1 in CD4+ T cells and promotes HIV latency reversal. ***J Clin Invest* 133**.DOI: https://doi.org/10.1172/jci164317, PMID: 37079384

PIERSON, T., MCARTHUR, J. & SILICIANO, R. F. 2000. Reservoirs for HIV-1: mechanisms for viral persistence in the presence of antiviral immune responses and antiretroviral therapy. ***Annu Rev Immunol* 18**: 665.DOI: https://doi.org/10.1146/annurev.immunol.18.1.665, PMID: 10837072

POH, A. 2016. First Oncolytic Viral Therapy for Melanoma. ***Cancer Discov* 6**: 6.DOI: https://doi.org/10.1158/2159-8290.Cd-nb2015-158, PMID: 26552414

RAWAT, P. & MITRA, D. 2011. Cellular heat shock factor 1 positively regulates human immunodeficiency virus-1 gene expression and replication by two distinct pathways. ***Nucleic Acids Res* 39**: 5879.DOI: https://doi.org/10.1093/nar/gkr198, PMID: 21459854

SUN, C., CHEN, Z., TANG, X., ZHANG, Y., FENG, L., DU, Y., XIAO, L., LIU, L., ZHU, W., CHEN, L. & ZHANG, L. 2013. Mucosal priming with a replicating-vaccinia virus-based vaccine elicits protective immunity to simian immunodeficiency virus challenge in rhesus monkeys. ***J Virol* 87**: 5669.DOI: https://doi.org/10.1128/jvi.03247-12, PMID: 23487457

SUN, C., FENG, L., ZHANG, Y., XIAO, L., PAN, W., LI, C., ZHANG, L. & CHEN, L. 2012. Circumventing antivector immunity by using adenovirus-infected blood cells for repeated application of adenovirus-vectored vaccines: proof of concept in rhesus macaques. ***J Virol* 86**: 11031.DOI: https://doi.org/10.1128/jvi.00783-12, PMID: 22855499

SUN, C., ZHANG, L., ZHANG, M., LIU, Y., ZHONG, M., MA, X. & CHEN, L. 2010. Induction of balance and breadth in the immune response is beneficial for the control of SIVmac239 replication in rhesus monkeys. ***J Infect* 60**: 371.DOI: https://doi.org/10.1016/j.jinf.2010.03.005, PMID: 20227437

SUN, C., ZUO, T. & WEN, Z. 2023a. B cell engineering in vivo: Accelerating induction of broadly neutralizing antibodies against HIV-1 infection. ***Signal Transduct Target Ther* 8**: 13.DOI: https://doi.org/10.1038/s41392-022-01269-4, PMID: 36604417

SUN, C., ZUO, T. & WEN, Z. 2023b. First clinical study of germline-targeting strategy: One step closer to a successful bnAb-based HIV vaccine. ***Innovation (Camb)* 4**: 100374.DOI: https://doi.org/10.1016/j.xinn.2023.100374, PMID: 36747593

TIMMONS, A., FRAY, E., KUMAR, M., WU, F., DAI, W., BULLEN, C. K., KIM, P., HETZEL, C., YANG, C., BEG, S., LAI, J., POMERANTZ, J. L., YUKL, S. A., SILICIANO, J. D. & SILICIANO, R. F. 2020. HSF1 inhibition attenuates HIV-1 latency reversal mediated by several candidate LRAs In Vitro and Ex Vivo. ***Proc Natl Acad Sci U S A* 117**: 15763.DOI: https://doi.org/10.1073/pnas.1916290117, PMID: 32571938

TRAUTMANN, L., JANBAZIAN, L., CHOMONT, N., SAID, E. A., GIMMIG, S., BESSETTE, B., BOULASSEL, M. R., DELWART, E., SEPULVEDA, H., BALDERAS, R. S., ROUTY, J. P., HADDAD, E. K. & SEKALY, R. P. 2006. Upregulation of PD-1 expression on HIV-specific CD8+ T cells leads to reversible immune dysfunction. ***Nat Med* 12**: 1198.DOI: https://doi.org/10.1038/nm1482, PMID: 16917489

VLACH, J. & PITHA, P. M. 1993. Differential contribution of herpes simplex virus type 1 gene products and cellular factors to the activation of human immunodeficiency virus type 1 provirus. ***J Virol* 67**: 4427.DOI: https://doi.org/10.1128/jvi.67.7.4427-4431.1993, PMID:

834 8389940
835 VLACH, J. & PITHA, P. M. 1992. Herpes simplex virus type 1-mediated induction of human
836 immunodeficiency virus type 1 provirus correlates with binding of nuclear proteins to the
837 NF-kappa B enhancer and leader sequence. ***J Virol* 66**: 3616.DOI:
838 https://doi.org/10.1128/jvi.66.6.3616-3623.1992, PMID: 1316471
839 WALKER-SPERLING, V. E. K., MERCADO, N. B., CHANDRASHEKAR, A., BORDUCCHI, E. N.,
840 LIU, J., NKOLOLA, J. P., LEWIS, M., MURRY, J. P., YANG, Y., GELEZIUNAS, R., ROBB,
841 M. L., MICHAEL, N. L., PAU, M. G., WEGMANN, F., SCHUITEMAKER, H., FRAY, E. J.,
842 KUMAR, M. R., SILICIANO, J. D., SILICIANO, R. F. & BAROUCH, D. H. 2022. Therapeutic
843 efficacy of combined active and passive immunization in ART-suppressed, SHIV-infected
844 rhesus macaques. ***Nat Commun* 13**: 3463.DOI: https://doi.org/10.1038/s41467-022-
845 31196-5, PMID: 35710819
846 WU, C., HE, Y., ZHAO, J., LUO, K., WEN, Z., ZHANG, Y., LI, M., CUI, Y., LIU, Z., WANG, C., HAN,
847 Z., LI, G., FENG, F., LI, P., CHEN, L. & SUN, C. 2022. Exacerbated AIDS Progression by
848 PD-1 Blockade during Therapeutic Vaccination in Chronically Simian Immunodeficiency
849 Virus-Infected Rhesus Macaques after Interruption of Antiretroviral Therapy. ***J Virol* 96**:
850 e0178521.DOI: https://doi.org/10.1128/JVI.01785-21, PMID: 34818070
851 WU, C., ZHAO, J., LI, R., FENG, F., HE, Y., LI, Y., HUANG, R., LI, G., YANG, H., CHENG, G.,
852 CHEN, L., MA, F., LI, P. & SUN, C. 2021. Modulation of Antiviral Immunity and Therapeutic
853 Efficacy by 25-Hydroxycholesterol in Chronically SIV-Infected, ART-Treated Rhesus
854 Macaques. ***Virol Sin* 36**: 1197.DOI: https://doi.org/10.1007/s12250-021-00407-6, PMID:
855 34057681
856 XIAO, L., WANG, D., SUN, C., LI, P., JIN, Y., FENG, L. & CHEN, L. 2014. Enhancement of SIV-
857 specific cell mediated immune responses by co-administration of soluble PD-1 and Tim-3
858 as molecular adjuvants in mice. ***Hum Vaccin Immunother* 10**: 724.DOI:
859 https://doi.org/10.4161/hv.27340, PMID: 24326266
860 XU, X., LIN, Y., ZENG, X., YANG, C., DUAN, S., DING, L., LU, W., LIN, J., PAN, X., MA, X. & LIU,
861 S. 2022. PARP1 Might Substitute HSF1 to Reactivate Latent HIV-1 by Binding to Heat
862 Shock Element. ***Cells* 11**.DOI: https://doi.org/10.3390/cells11152331, PMID: 35954175
863 YANG, Q., FENG, F., LI, P., PAN, E., WU, C., HE, Y., ZHANG, F., ZHAO, J., LI, R., FENG, L., HU,
864 F., LI, L., ZOU, H., CAI, W., LEHNER, T., SUN, C. & CHEN, L. 2019. Arsenic Trioxide
865 Impacts Viral Latency and Delays Viral Rebound after Termination of ART in Chronically
866 SIV-Infected Macaques. ***Adv Sci (Weinh)* 6**: 1900319.DOI:
867 https://doi.org/10.1002/advs.201900319, PMID: 31380187
868 YEH, Y. J. & HO, Y. C. 2021. Shock-and-kill versus block-and-lock: Targeting the fluctuating and
869 heterogeneous HIV-1 gene expression. ***Proc Natl Acad Sci U S A* 118**.DOI:
870 https://doi.org/10.1073/pnas.2103692118, PMID: 33758027
871 ZENG, X., PAN, X., XU, X., LIN, J., QUE, F., TIAN, Y., LI, L. & LIU, S. 2017. Resveratrol Reactivates
872 Latent HIV through Increasing Histone Acetylation and Activating Heat Shock Factor 1. ***J
873 Agric Food Chem* 65**: 4384.DOI: https://doi.org/10.1021/acs.jafc.7b00418, PMID:
874 28471170
875 ZHAO, J., CHEN, J., WANG, C., LIU, Y., LI, M., LI, Y., LI, R., HAN, Z., WANG, J., CHEN, L., SHU,
876 Y., CHENG, G. & SUN, C. 2022. Kynurenine-3-monooxygenase (KMO) broadly inhibits
877 viral infections via triggering NMDAR/Ca2+ influx and CaMKII/ IRF3-mediated IFN-beta
878 production. ***PLoS Pathog* 18**: e1010366.DOI:
879 https://doi.org/10.1371/journal.ppat.1010366, PMID: 35235615
880 ZHOU, J., CHEUNG, A. K., TAN, Z., WANG, H., YU, W., DU, Y., KANG, Y., LU, X., LIU, L., YUEN,
881 K. Y. & CHEN, Z. 2013. PD1-based DNA vaccine amplifies HIV-1 GAG-specific CD8+ T
882 cells in mice. ***J Clin Invest* 123**: 2629.DOI: https://doi.org/10.1172/jci64704, PMID:
883 23635778
884

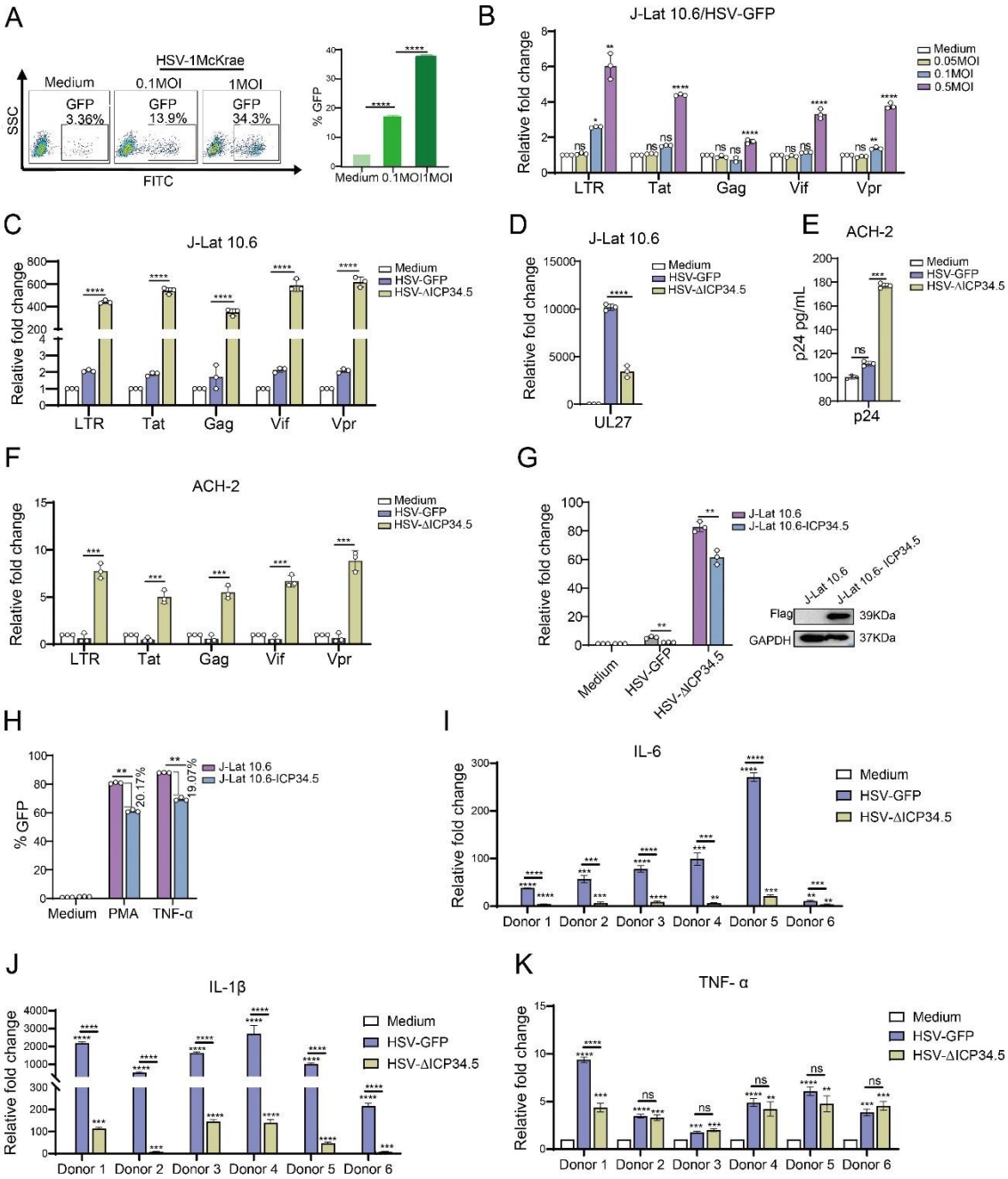

Figure 1. The modified HSV-ΔICP34.5-based constructs reactivated HIV latency more efficiently than wild-type HSV counterparts. (**A**) J-Lat 10.6 cells (1×10^6) were infected with varying MOIs of wild-type HSV-1 Mckrae strain for 30 h. The proportion of GFP+ cells, indicating activated latent cells, is shown in the pseudocolor plot (left) and the corresponding bar chart (right). (**B**) J-Lat 10.6 cells (1×10^6) were infected with varying MOIs of HSV-1 17 strain containing GFP (HSV-GFP) for 30 h, and the mRNA levels of HIV-1 transcripts driven by the 5' LTR, as well as Tat, Gag, Vpr, and Vif, are presented in the histogram. (**C**)J-Lat 10.6 cells (1×10^6) were infected with HSV-GFP or HSV-ΔICP34.5 at an MOI of 0.1 for 30 h.

The mRNA levels of HIV-1 transcripts driven by the 5' LTR, as well as Tat, Gag, Vpr, Vif, and (**D**) HSV-1 UL27 are presented in the histogram. (**E**) ACH-2 cells (1×10^6) were infected with HSV-GFP or HSV-ΔICP34.5 at an MOI of 0.1 for 30 h. The p24 protein level was detected using an HIV-1 p24 ELISA kit, and the mRNA levels of HIV-1 transcripts driven by the 5' LTR, as well as Tat, Gag, Vpr, and Vif, are shown in the histogram (**F**). (**G**) J-Lat 10.6 and J-Lat 10.6-ICP34.5 cells were infected with HSV-GFP or HSV-ΔICP34.5, and the mRNA levels of HIV-1 Tat were shown with the histogram (left). Blotting showed that J-Lat 10.6 cells stably expressing HSV ICP34.5 (J-Lat 10.6-ICP34.5) can appropriately express ICP34.5 protein using Flag-tag antibodies (right). (**H**) J-Lat 10.6 and J-Lat 10.6-ICP34.5 cells were respectively stimulated with PMA (10 ng/mL) and TNF-α (10 ng/mL), and the expression level of GFP^+ cells is displayed with the corresponding bar chart. (**I-K**) Primary $CD4^+$ T cells from people living with HIV (PLWH) were infected with HSV-GFP or HSV-ΔICP34.5. The inflammatory response was assessed by evaluating mRNA levels of IL-6, IL-1β and TNF-α using qPCR. Data shown are mean ± SD. $^{**}P<0.01$, $^{***}P<0.001$, $^{****}P<0.0001$. ns: no significance.

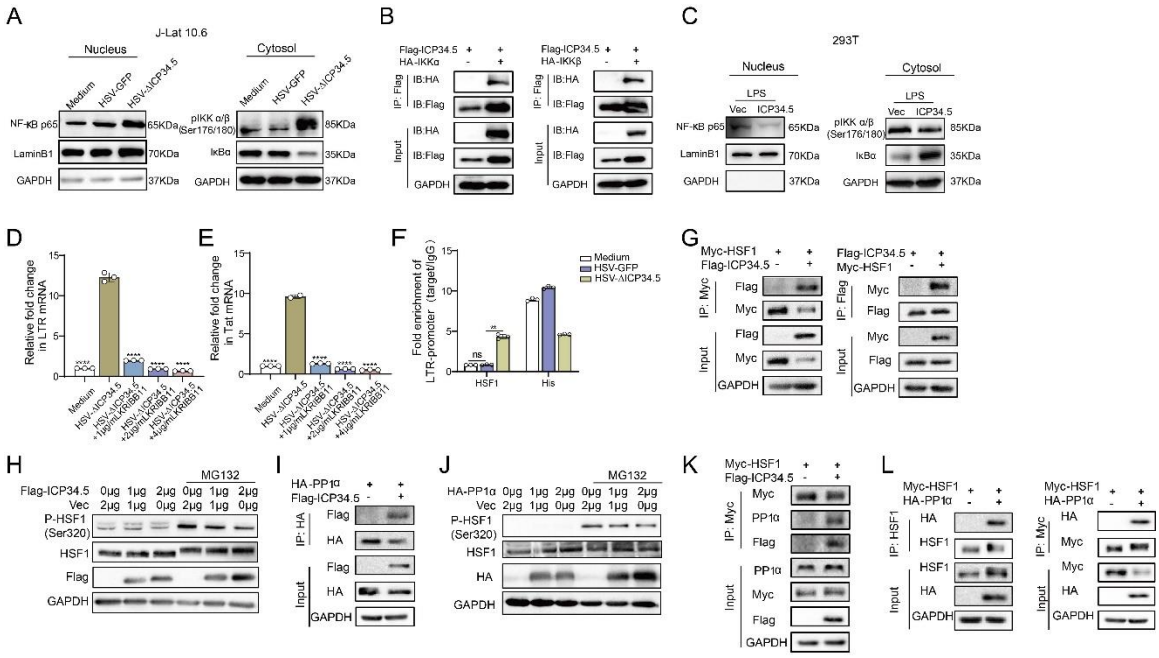

Figure 2. The modified HSV-based constructs effectively reactivated HIV latency by modulating the NF-κB pathway and HSF1 pathway. (**A**) J-Lat 10.6 cells infected with HSV-GFP and HSV-ΔICP34.5 at MOI 0.1. Cytoplasmic and nuclear proteins were analyzed for p65, p-IKKα/β and IkBα levels. GAPDH and Lamin B1 served as loading controls for cytoplasmic and nuclear proteins, respectively. (**B**) 293T cells transfected with Flag-ICP34.5, IKKα (left), or IKKβ (right) analyzed through Co-IP assays. (**C**) 293T cells were transfected with Flag-ICP34.5 or empty vector (Vec) for 24h, treated with LPS (1μg/mL) for 8h. Cytoplasmic and nuclear proteins analyzed by Western blot (WB). (**D-E**) J-Lat 10.6 cells infected with HSV-ΔICP34.5 treated with various KRIBB11 concentrations. Levels of mRNA for Tat and HIV-1 transcripts driven by the 5' LTR were analyzed by qPCR. (**F**) J-Lat 10.6 cells infected with HSV-wt or HSV-ΔICP34.5 at MOI 0.1 for 36h. ChIP-qPCR assessed HSF1 binding to LTR. IgG and Histone antibody (His) served as negative and positive controls. (**G**) 293T cellstransfected with Flag-ICP34.5 and Myc-HSF1, analyzed by Co-IP assays. (**H**) The immunoblot depicts the alterations in protein levels in 293T cells transfected with either empty vector or ICP34.5 for 6 h, followed by 24 h of treatment with 10 μM MG132. (**I**) 293T cells transfected with Flag-ICP34.5 and HA-PP1α, analyzed by Co-IP assays. (**J**) The immunoblot depicts the alterations in protein levels in 293T cells transfected with either empty vector or HA-PP1α for 6 h, followed by 24 h of treatment with 10 μM MG132. (**K**) 293T cells transfected with Myc-HSF1 with or without Flag-ICP34.5, analyzed by Co-IP assays. (**L**) 293T cells transfected with Myc-HSF1 and HA-PP1α, analyzed through Co-IP assays. Data shown are mean ± SD. ***P*<0.01, ****P<0.0001. ns: no significance.

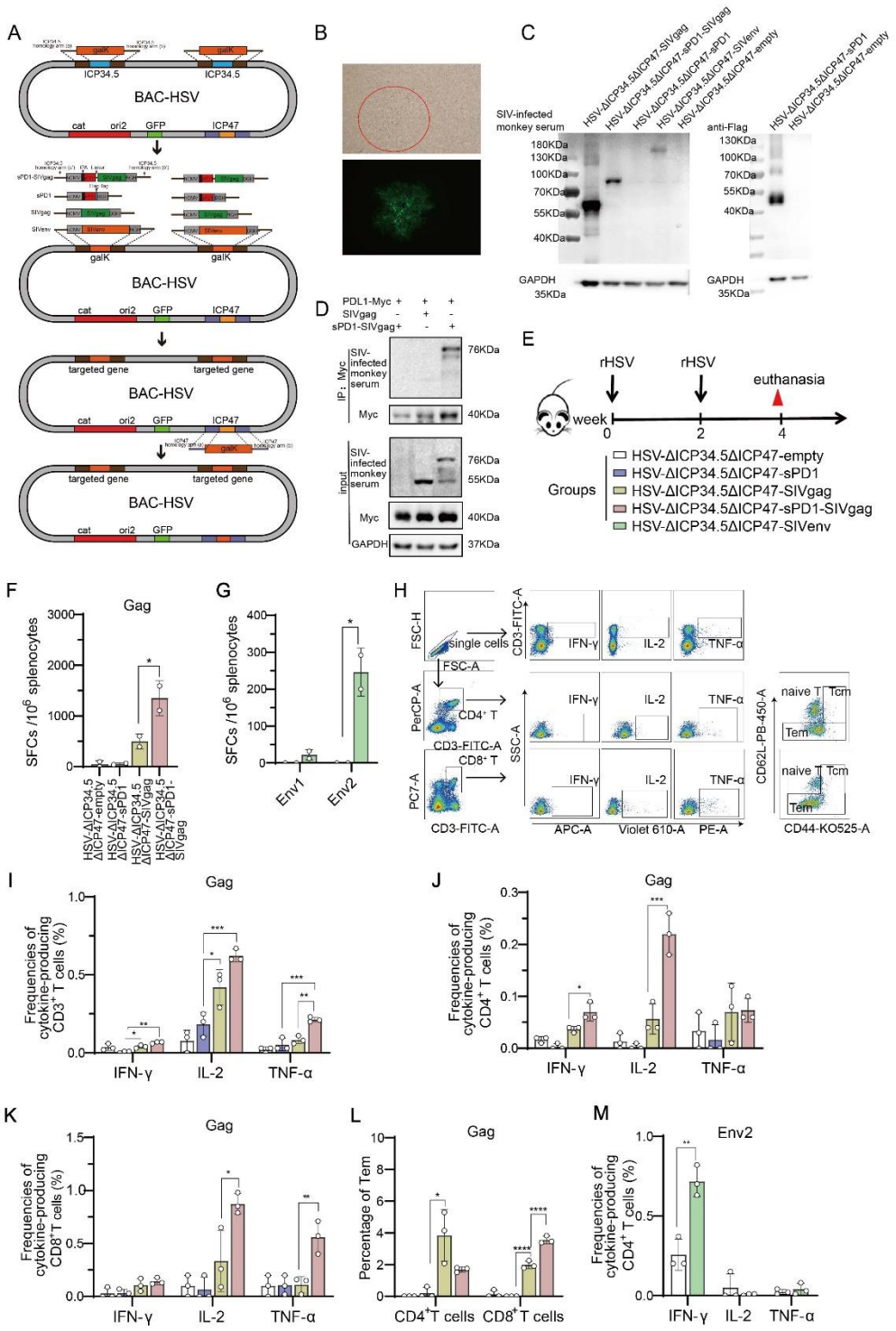

Figure 3. Recombinant HSV-1 vector-based SIV vaccines induce specific T cell immune responses in mice. (**A**) Schematic diagram illustrating the construction of recombinant HSV through the BAC/galK selection system. The

ICP34.5 gene was replaced with the galK gene via homologous recombination, followed by substituting galK with a target gene expression cassette containing the hCMV promoter and BGH terminator. Finally, the ICP47 gene was deleted. (**B**) Brightfield (top) and fluorescence (bottom) images of a clone of the rescued recombinant HSV. (**C**) Vero cells infected with recombinant HSV constructs, with protein expression of targeted genes detected using SIV-infected monkey serum. (**D**) HeLa cells transfected with Myc-PDL1 and then infected with HSV-ΔICP34.5ΔICP47-empty, HSV-ΔICP34.5ΔICP47-SIVgag, or HSV-ΔICP34.5ΔICP47-sPD1-SIVgag at an MOI of 0.1 for 24 h. Cell lysates were subjected to Co-IP analysis. (**E**) Schematic schedule of mouse vaccination. Twenty-five mice were randomly allocated to five groups: HSV-ΔICP34.5ΔICP47-empty, HSV-ΔICP34.5ΔICP47-sPD1, HSV-ΔICP34.5ΔICP47-SIVgag, HSV-ΔICP34.5ΔICP47-sPD1-SIVgag, and HSV-ΔICP34.5ΔICP47-SIVenv. Mice were injected with the corresponding vaccines at weeks 0 and 2. At week 4, mice were sacrificed, and spleen lymphocytes were collected to evaluate immune response.(**F-G**) Column graphs showing the number of Gag or Env1, Env2-specific spot-forming cells (SFCs) per 10^6 spleen lymphocytes, as measured by IFN-γ ELISpot assay. (**H**) Pseudocolor plot of flow cytometry illustrating the gating strategy. Column graphs showing the frequencies of IFN-γ, IL-2, and TNF-α production from gag-specific $CD3^+$ T (**I**), $CD4^+$ T (**J**), and $CD8^+$ T cells (**K**). (**L**) Bar chart showing the proportion of Tem (effector memory T cells) among $CD4^+$ T and $CD8^+$ T cells upon stimulation with the SIV Gag peptide pools.(**M**) Bar chart showing the frequencies of Env2-specific IFN-γ^+ $CD4^+$ T cells. Data were expressed as mean ± SD from five mice samples. Three independent experiments for the animal immunization were repeated. *P<0.05, **P<0.01, ***P<0.001, ****P<0.0001. ns: no significance.

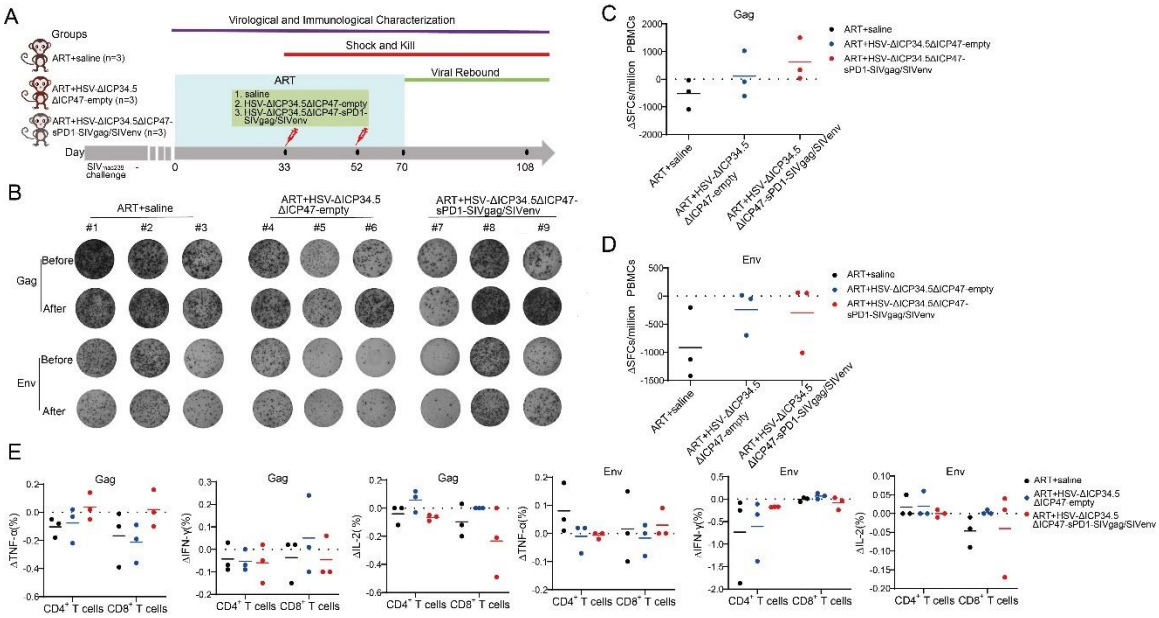

Figure 4. The modified HSV-based constructs efficiently elicited SIV-specific immune responses in chronically SIV-infected macaques. (**A**) Schematic schedule of the macaque experiment. Nine chronically SIV-infected macaques were assigned into three groups: ART+saline group (n=3), ART+HSV-ΔICP34.5ΔICP47-empty group (n=3), and ART+HSV-ΔICP34.5ΔICP47-sPD1-SIVgag/SIVenv group (n=3). All SIV-infected macaques received ART treatment (FTC/6.7 mg/kg/once daily, PMPA/10 mg/kg/once daily) for 33 days. On days 33 and 52, macaques were immunized with saline, HSV-ΔICP34.5ΔICP47-empty, and HSV-ΔICP34.5ΔICP47-sPD1-SIVgag/SIVenv respectively. ART treatment ,was interrupted in all macaques on day 70 after the second vaccination. Samples were collected at various time points to monitor virological and immunological parameters. (**B**) Representative images of Gag or Env-specific spots (2.5×10^5 cells per well) from each macaque pre-vaccination (before, day 33) and post-vaccination (after, day 70) by ELISpot assay. (**C-D**) Difference in SIV-specific IFN-γ-secreting cells (ΔSFCs) between pre- and post-immunization, assessing the immune response induced by HSV-ΔICP34.5ΔICP47-vectored SIV vaccines. (**E**) Difference in SIV-specific TNF-α/IFN-γ/IL-2-secreting $CD4^+$ T and $CD8^+$ T subsets between pre- and post-immunization, detected by ICS assay.

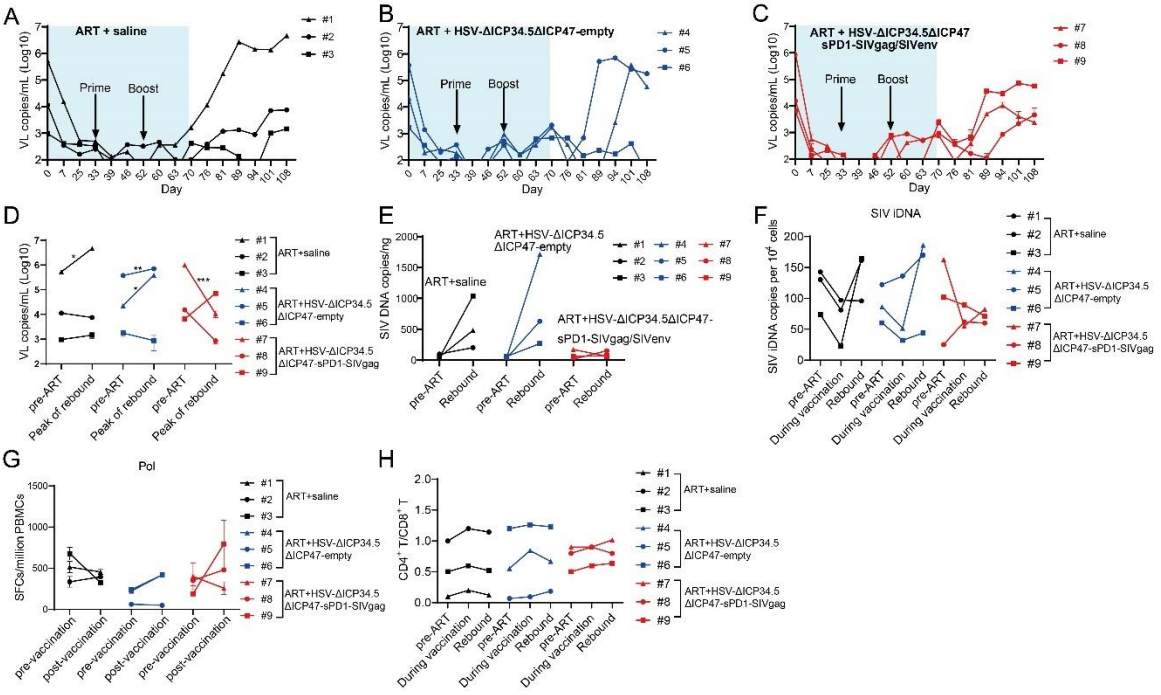
A
ART + saline
Prime
Boost
VL copies/mL (Log10)
Day
#1
#2
#3
B
ART + HSV-ΔICP34.5ΔICP47-empty
#4
#5
#6
C
ART + HSV-ΔICP34.5ΔICP47
sPD1-SIVgag/SIVenv
#7
#8
#9
D
ART+saline
ART+HSV-ΔICP34.5
ΔICP47-empty
ART+HSV-ΔICP34.5
ΔICP47-sPD1-SIVgag
pre-ART
Peak of rebound
E
SIV DNA copies/ng
ART+HSV-ΔICP34.5
ΔICP47-empty
ART+saline
ART+HSV-ΔICP34.5ΔICP47-
sPD1-SIVgag/SIVenv
Rebound
F
SIV iDNA
SIV iDNA copies per 10^4 cells
During vaccination
G
Pol
SFCs/million PBMCs
pre-vaccination
post-vaccination
H
CD4+ T/CD8+ T

990

Figure 5. The modified HSV-based constructs effectively reactivated SIV latency in vivo in chronically SIV-infected, ART-treated macaques. (**A-C**) Viral load (VL) changes in plasma for each animal were monitored throughout the experiment using real-time PCR. The detection limit is 100 copies per mL plasma. The shaded area represented the duration of ART administration. (**D**) The VL change in plasma between pre-ART and the peak value in the rebound stage after ART discontinuation. (**E**) Change in total SIV DNA copies between pre-ART and viral rebound after ART discontinuation. (**F**) SIV integrated DNA (iDNA) copy numbers detected by Alu-PCR at different time points. (**G**) Change in the number of SIV Pol-specific IFN-γ-secreting cells between pre-immunization (day 33) and post-immunization (day 70), asdetected by ELISpot assay. (**H**) Change in the $CD4^+$ T/ $CD8^+$ T ratio. Data shown are mean ± SD. ***P*<0.01, ****P*<0.0001, *****P*<0.0001.

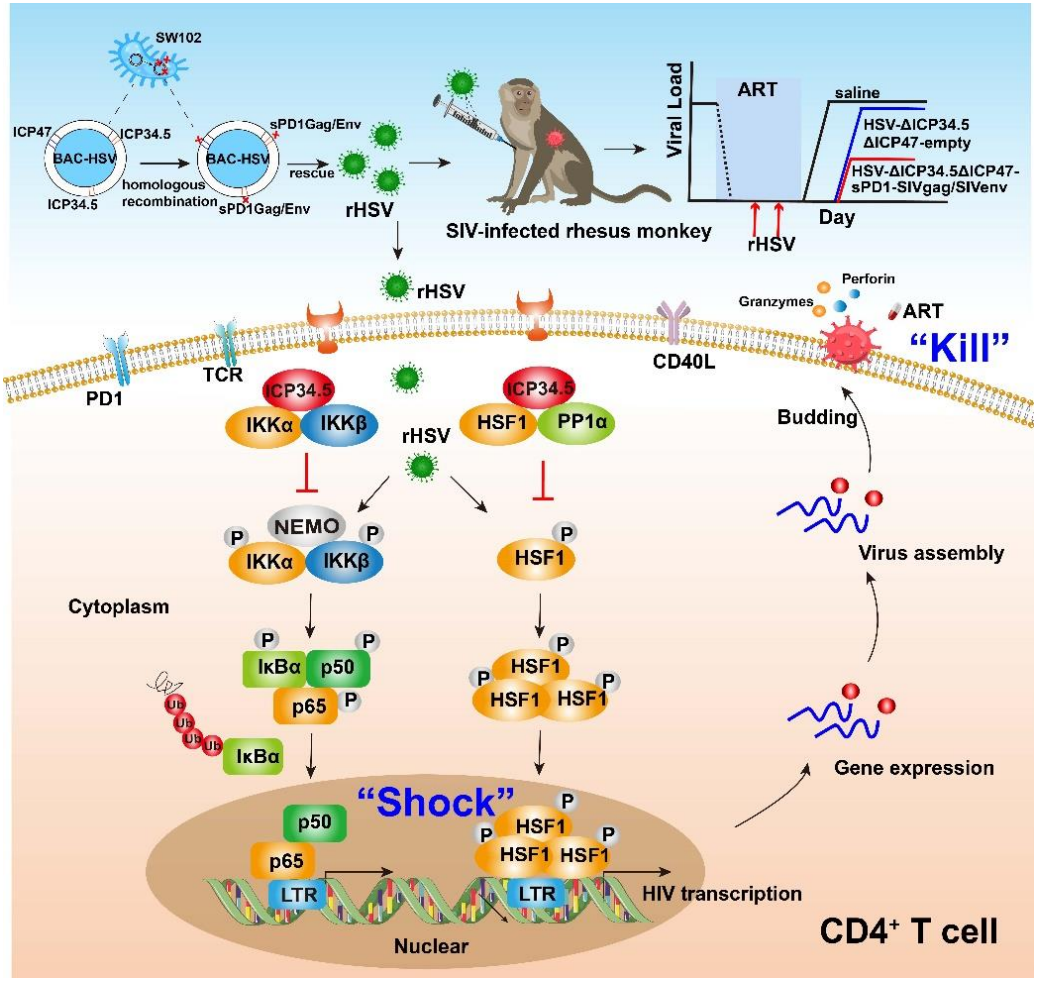

Figure 6. Pattern to illustrate the proof-of-concept strategy based on a bifunctional HSV-ΔICP34.5-vectored therapeutic vaccine for HIV functional cure. In the present study, the modified HSV-ΔICP34.5-based constructs

effectively reactivated HIV/SIV latency by modulating the IKKα/β-NF-κB pathway and PP1-HSF1 pathway (Shock) and simultaneously elicited antigen-specific polyfunctional $CD8^+$ T cells to eliminate cells infected with the reactivated virion (Kill). BAC: bacterial artificial chromosome; rHSV: recombinant HSV; TCR: T-cell receptor; PD1: Programmed Cell Death Protein 1; CD40L: CD40 Ligand.

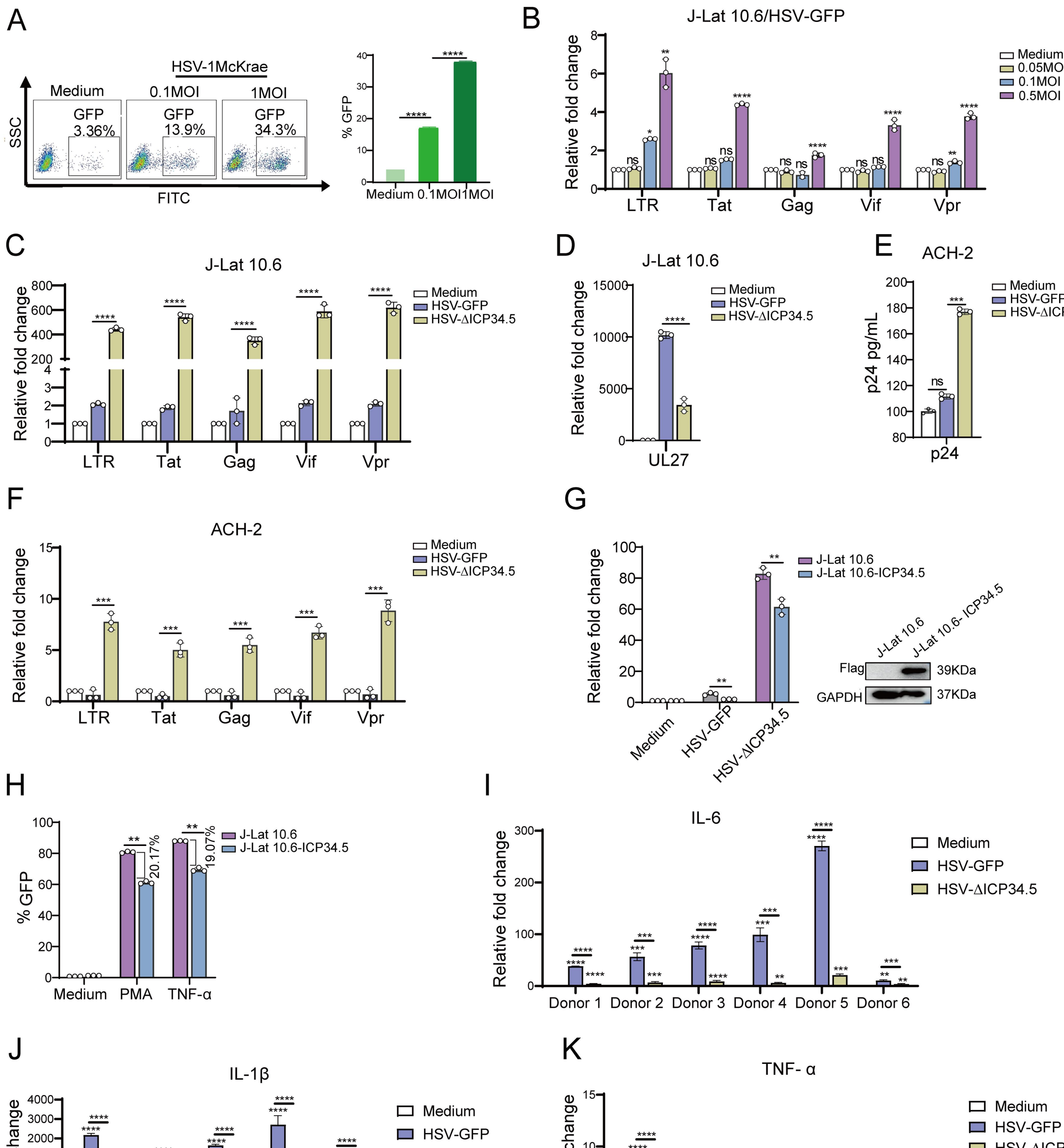
A
HSV-1McKrae
Medium
0.1MOI
1MOI
GFP 3.36%
GFP 13.9%
GFP 34.3%
SSC
FITC
% GFP
Medium 0.1MOI 1MOI
B
J-Lat 10.6/HSV-GFP
Relative fold change
Medium
0.05MOI
0.1MOI
0.5MOI
LTR
Tat
Gag
Vif
Vpr
C
J-Lat 10.6
Relative fold change
Medium
HSV-GFP
HSV-ΔICP34.5
LTR
Tat
Gag
Vif
Vpr
D
J-Lat 10.6
Relative fold change
Medium
HSV-GFP
HSV-ΔICP34.5
UL27
E
ACH-2
p24 pg/mL
Medium
HSV-GFP
HSV-ΔICP34.5
p24
F
ACH-2
Relative fold change
Medium
HSV-GFP
HSV-ΔICP34.5
LTR
Tat
Gag
Vif
Vpr
G
Relative fold change
J-Lat 10.6
J-Lat 10.6-ICP34.5
Medium
HSV-GFP
HSV-ΔICP34.5
J-Lat 10.6
J-Lat 10.6- ICP34.5
Flag
39KDa
GAPDH
37KDa
H
% GFP
J-Lat 10.6
J-Lat 10.6-ICP34.5
20.17%
19.07%
Medium
PMA
TNF-α
I
IL-6
Relative fold change
Medium
HSV-GFP
HSV-ΔICP34.5
Donor 1
Donor 2
Donor 3
Donor 4
Donor 5
Donor 6
J
IL-1β
Medium
HSV-GFP
K
TNF- α
Medium
HSV-GFP

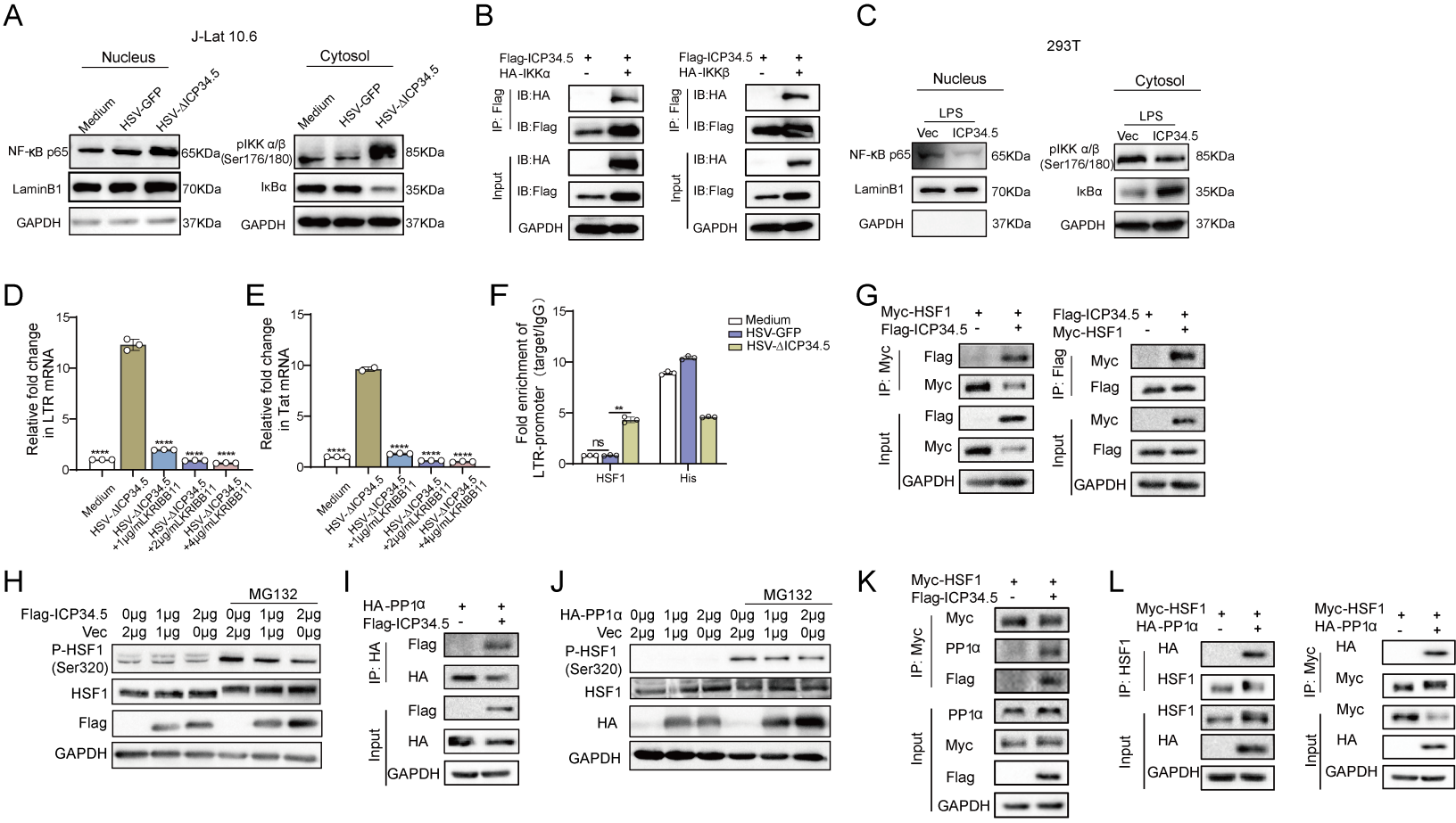
A
J-Lat 10.6
Nucleus
Cytosol
Medium
HSV-GFP
HSV-ΔICP34.5
NF-κB p65
LaminB1
GAPDH
65KDa
70KDa
37KDa
pIKK α/β (Ser176/180)
IκBα
85KDa
35KDa
B
Flag-ICP34.5
HA-IKKα
HA-IKKβ
IP: Flag
Input
IB:HA
IB:Flag
C
293T
LPS
Vec
ICP34.5
D
Relative fold change in LTR mRNA
HSV-ΔICP34.5 +1μg/mLKRIBB11
HSV-ΔICP34.5 +2μg/mLKRIBB11
HSV-ΔICP34.5 +4μg/mLKRIBB11
E
Relative fold change in Tat mRNA
F
Fold enrichment of LTR-promoter（target/IgG）
Medium
HSV-GFP
HSV-ΔICP34.5
HSF1
His
ns
G
Myc-HSF1
Flag-ICP34.5
IP: Myc
IP: Flag
Flag
Myc
GAPDH
H
MG132
Vec
P-HSF1 (Ser320)
HSF1
I
HA-PP1α
J
K
PP1α
L
IP: HSF1
IP: Myc
HA

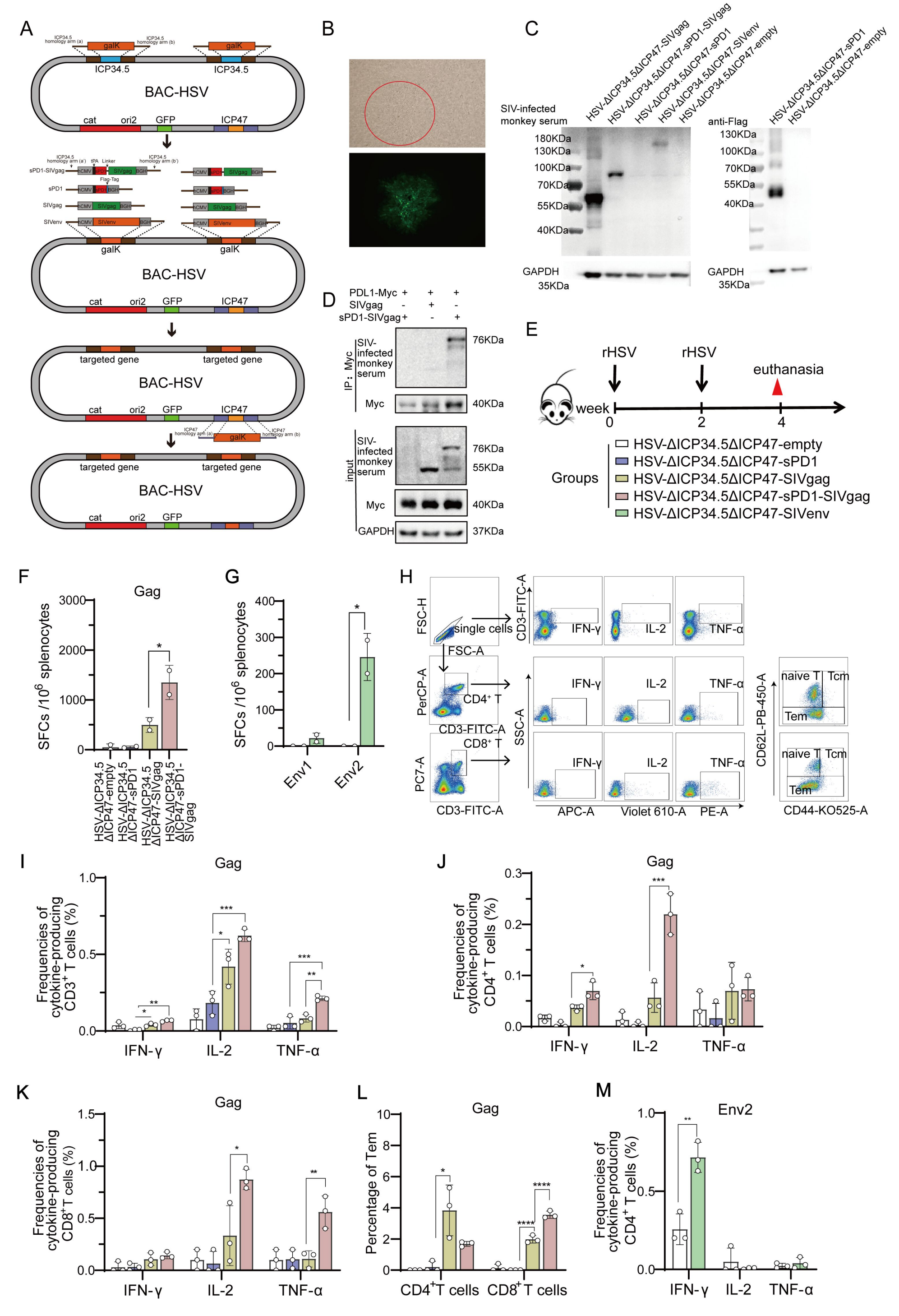
A
ICP34.5 homology arm (a)
galK
ICP34.5 homology arm (b)
ICP34.5
BAC-HSV
cat
ori2
GFP
ICP47
sPD1-SIVgag
sPD1
SIVgag
SIVenv
tPA
Linker
Flag-Tag
hCMV
BGH
targeted gene
B
C
SIV-infected monkey serum
HSV-ΔICP34.5ΔICP47-SIVgag
HSV-ΔICP34.5ΔICP47-sPD1-SIVgag
HSV-ΔICP34.5ΔICP47-sPD1
HSV-ΔICP34.5ΔICP47-SIVenv
HSV-ΔICP34.5ΔICP47-empty
anti-Flag
180KDa
130KDa
100KDa
70KDa
55KDa
40KDa
GAPDH
35KDa
D
PDL1-Myc
SIVgag
sPD1-SIVgag
IP: Myc
input
Myc
76KDa
55KDa
40KDa
37KDa
E
rHSV
euthanasia
week
0
2
4
Groups
HSV-ΔICP34.5ΔICP47-empty
HSV-ΔICP34.5ΔICP47-sPD1
HSV-ΔICP34.5ΔICP47-SIVgag
HSV-ΔICP34.5ΔICP47-sPD1-SIVgag
HSV-ΔICP34.5ΔICP47-SIVenv
F
Gag
SFCs /10^6 splenocytes
HSV-ΔICP34.5 ΔICP47-empty
HSV-ΔICP34.5 ΔICP47-sPD1
HSV-ΔICP34.5 ΔICP47-SIVgag
HSV-ΔICP34.5 ΔICP47-sPD1-SIVgag
G
Env1
Env2
H
FSC-H
single cells
FSC-A
PerCP-A
CD4+ T
CD3-FITC-A
PC7-A
CD8+ T
CD3-FITC-A
SSC-A
IFN-γ
IL-2
TNF-α
APC-A
Violet 610-A
PE-A
CD62L-PB-450-A
naive T
Tcm
Tem
CD44-KO525-A
I
Frequencies of cytokine-producing CD3+ T cells (%)
J
Frequencies of cytokine-producing CD4+ T cells (%)
K
Frequencies of cytokine-producing CD8+ T cells (%)
L
Percentage of Tem
CD4+T cells
CD8+T cells
M
Env2

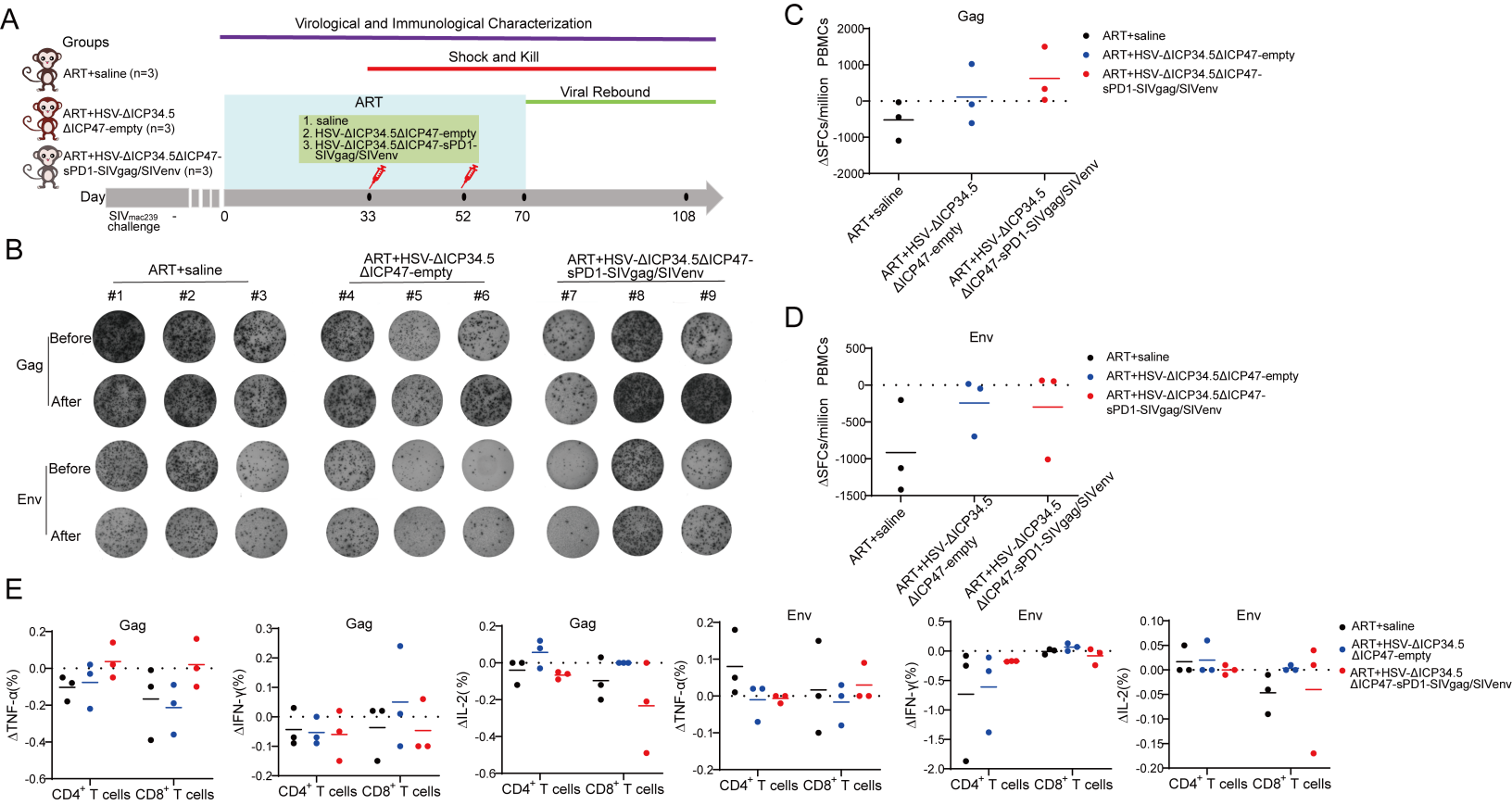
A
Groups
ART+saline (n=3)
ART+HSV-ΔICP34.5 ΔICP47-empty (n=3)
ART+HSV-ΔICP34.5ΔICP47-sPD1-SIVgag/SIVenv (n=3)
Virological and Immunological Characterization
Shock and Kill
Viral Rebound
ART
1. saline
2. HSV-ΔICP34.5ΔICP47-empty
3. HSV-ΔICP34.5ΔICP47-sPD1-SIVgag/SIVenv
Day
SIVmac239 challenge
-
0
33
52
70
108
B
ART+saline
ART+HSV-ΔICP34.5 ΔICP47-empty
ART+HSV-ΔICP34.5ΔICP47-sPD1-SIVgag/SIVenv
#1
#2
#3
#4
#5
#6
#7
#8
#9
Gag
Before
After
Env
Before
After
C
Gag
ΔSFCs/million PBMCs
2000
1000
0
-1000
-2000
ART+saline
ART+HSV-ΔICP34.5 ΔICP47-empty
ART+HSV-ΔICP34.5ΔICP47-sPD1-SIVgag/SIVenv
D
Env
ΔSFCs/million PBMCs
500
0
-500
-1000
-1500
ART+saline
ART+HSV-ΔICP34.5 ΔICP47-empty
ART+HSV-ΔICP34.5ΔICP47-sPD1-SIVgag/SIVenv
E
Gag
ΔTNF-α(%)
ΔIFN-γ(%)
ΔIL-2(%)
Env
ΔTNF-α(%)
ΔIFN-γ(%)
ΔIL-2(%)
CD4+ T cells
CD8+ T cells
ART+saline
ART+HSV-ΔICP34.5 ΔICP47-empty
ART+HSV-ΔICP34.5 ΔICP47-sPD1-SIVgag/SIVenv

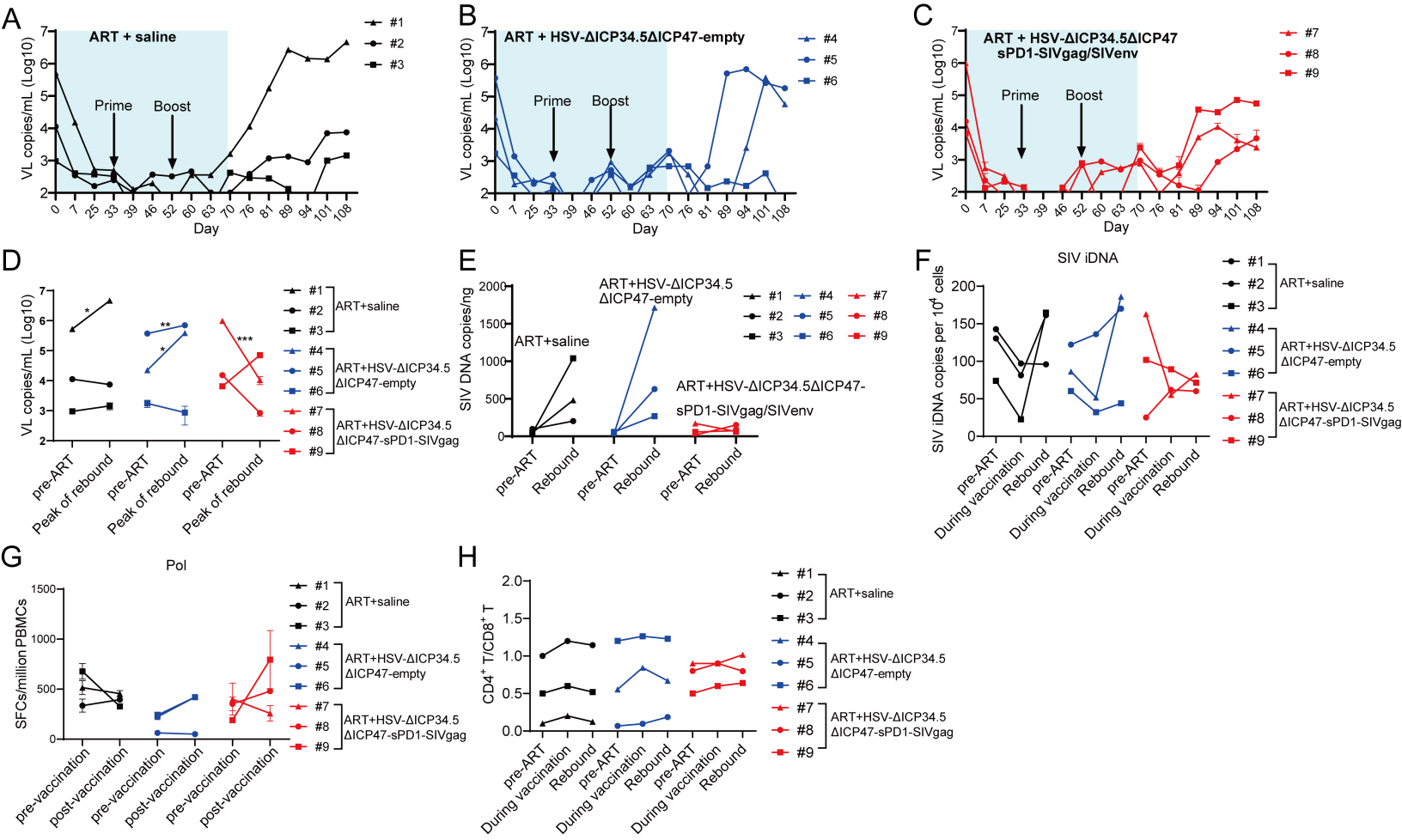
A
ART + saline
Prime
Boost
VL copies/mL (Log10)
Day
#1
#2
#3
B
ART + HSV-ΔICP34.5ΔICP47-empty
#4
#5
#6
C
ART + HSV-ΔICP34.5ΔICP47
sPD1-SIVgag/SIVenv
#7
#8
#9
D
ART+saline
ART+HSV-ΔICP34.5
ΔICP47-empty
ART+HSV-ΔICP34.5
ΔICP47-sPD1-SIVgag
pre-ART
Peak of rebound
E
SIV DNA copies/ng
ART+HSV-ΔICP34.5
ΔICP47-empty
ART+saline
ART+HSV-ΔICP34.5ΔICP47-
sPD1-SIVgag/SIVenv
Rebound
F
SIV iDNA
SIV iDNA copies per 10^4 cells
During vaccination
G
Pol
SFCs/million PBMCs
pre-vaccination
post-vaccination
H
CD4+ T/CD8+ T

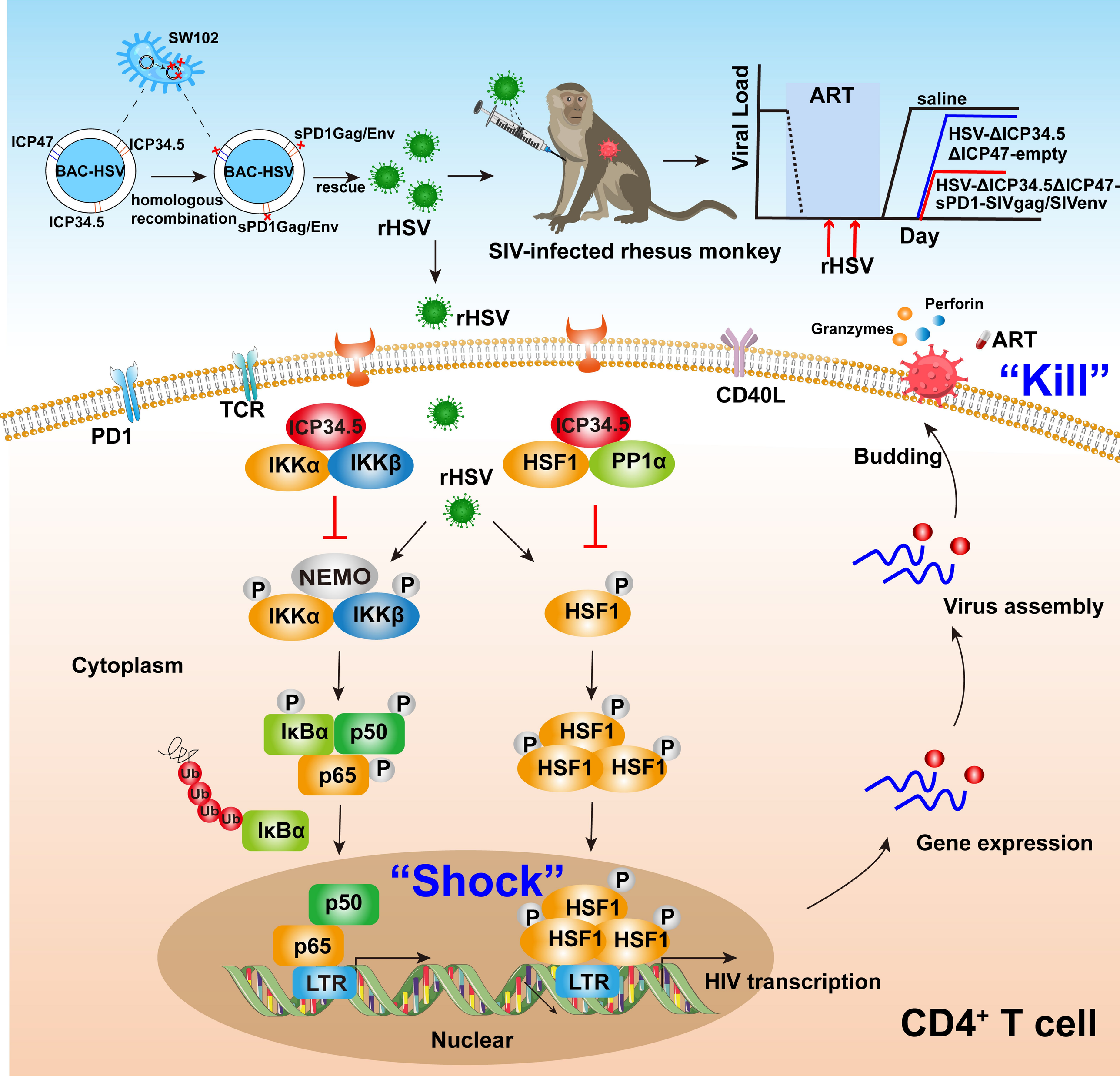
SW102
ICP47
ICP34.5
BAC-HSV
ICP34.5
homologous recombination
BAC-HSV
sPD1Gag/Env
sPD1Gag/Env
rescue
rHSV
SIV-infected rhesus monkey
Viral Load
ART
saline
HSV-ΔICP34.5 ΔICP47-empty
HSV-ΔICP34.5ΔICP47-sPD1-SIVgag/SIVenv
Day
rHSV
rHSV
Perforin
Granzymes
ART
"Kill"
PD1
TCR
CD40L
ICP34.5
IKKα
IKKβ
rHSV
ICP34.5
HSF1
PP1α
Budding
NEMO
P
IKKα
IKKβ
P
HSF1
P
Virus assembly
Cytoplasm
P
IκBα
p50
P
p65
P
HSF1
P
HSF1
HSF1
P
P
Ub
Ub
Ub
Ub
IκBα
Gene expression
"Shock"
p50
p65
LTR
P
HSF1
P
HSF1
HSF1
P
LTR
HIV transcription
Nuclear
CD4+ T cell